NASA Technical Memorandum 110392

Analytical Fuselage and Wing Weight Estimation of Transport Aircraft

Mark D. Ardema, Mark C. Chambers,
Anthony P. Patron, Andrew S. Hahn,
Hirokazu Miura, and Mark D. Moore

May 1996

National Aeronautics and
Space Administration

NASA Technical Memorandum 110392

Analytical Fuselage and Wing Weight Estimation of Transport Aircraft

Mark D. Ardema, Mark C. Chambers, and Anthony P. Patron, Santa Clara University, Santa Clara, California
Andrew S. Hahn, Hirokazu Miura, and Mark D. Moore, Ames Research Center, Moffett Field, California

May 1996

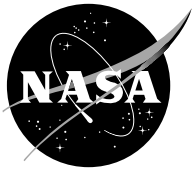

National Aeronautics and Space Administration

Ames Research Center
Moffett Field, California 94035-1000

Nomenclature

A	fuselage cross-sectional area
A_B	fuselage surface area
A_F	frame cross-sectional area
(AR)	aspect ratio of wing
b	wingspan; intercept of regression line
b_s	stiffener spacing
b_S	wing structural semispan, measured along quarter chord from fuselage
b_w	stiffener depth
C_F	Shanley's constant
C_P	center of pressure
C_R	root chord of wing at fuselage intersection
C'_R	theoretical root chord of wing
C_{s_1}	portion of wing leading edge not used for structural box
C_{s_2}	portion of wing trailing edge not used for structural box
C_{SR}	structural root chord of wing
C_{ST}	structural tip chord of wing
C_T	tip chord of wing
d	frame spacing
d_W	optimum web spacing of wing
D	maximum diameter of fuselage
e	wing buckling exponent
e_C	wing cover material factor
E	Young's modulus of shell material
E_F	Young's modulus of frame material
F_{cy}	compressive yield strength
F_S	shear strength
F_{tu}	ultimate tensile strength
h	thickness of sandwich shell
h_{e_i}	step function for ith engine on wing
h_{lg_i}	step function for ith landing gear on wing
I_F	frame cross-sectional area moment of inertia
I_y	area moment of inertia about the y-axis
I'_y	$I_y / \bar{t}_s$
K_{F1}	frame stiffness coefficient, I_F/A_F^2
K_{mg}	shell minimum gage factor
K_P	shell geometry factor for hoop stress
K_S	constant for shear stress in wing
K_{th}	sandwich thickness parameter
l_B	fuselage length
l_{LE}	length from leading edge to structural box at theoretical root chord
l_{MG}	length from nose to fuselage mounted main gear
l_{NG}	length from nose to nose gear
l_{TE}	length from trailing edge to structural box at theoretical root chord
l_1	length of nose portion of fuselage
l_2	length of tail portion of fuselage
l_π	length from nose to breakpoint of fuselage
L	lift
L_T	maximum vertical tail lift
m	buckling equation exponent; slope of regression line
M	longitudinal bending moment
n	normal load factor
n_x	longitudinal acceleration
N_{x_A}	axial stress resultant
N_{x_B}	bending stress resultant
N_{x_P}	pressure stress resultant
N_x^+	tensile axial stress resultant
N_x^-	compressive axial stress resultant
N_y	hoop direction stress resultant
P	perimeter
P_g	internal gage pressure
P_s	perimeter of shell
P_w	perimeter of walls
P_1	exponent of power law of nose section of fuselage
P_2	exponent of power law of tail section of fuselage
r	radius of fuselage

$r(y)$	total wing chord as a function of position along quarter chord
$r_s(y)$	structural wing chord as a function of position along quarter chord
R	correlation coefficient used for regression
R_{fin}	fineness ratio
R_{HT}	ratio of horizontal tail station to fuselage length
R_{LE}	ratio of wing leading edge station at theoretical root chord to fuselage length
R_{MG}	ratio of length to main gear to fuselage length
R_{NG}	ratio of length to nose gear to fuselage length
R_{P_1}	ratio of length to leading edge of fuselage mounted propulsion to fuselage length
R_{P2}	ratio of length to trailing edge of fuselage mounted propulsion to fuselage length
$R_t(y)$	thickness ratio of wing as a function of position along quarter chord
R_{TAP}	taper ratio of wing
S_B	plan area of the fuselage
S_{LG}	stroke of landing gear
S_P	plan area of wing
$t(y)$	thickness of wing box as a function of position along quarter chord
t_c	core thickness
t_f	face sheet thickness
t_g	material gage thickness, $\bar{t}_s / K_{mg}$
t_{mg}	material minimum gage thickness
t_s	skin thickness
t_w	stiffener thickness
$\bar{t}$	total equivalent isotropic thickness of shell and frames
$\bar{t}_B$	total equivalent isotropic thickness of fuselage structure
$\bar{t}_F$	smeared equivalent isotropic thickness of frames
$\bar{t}_S$	equivalent isotropic thickness of shell
$\bar{t}_{S_B}$	shell thickness required to preclude buckling failure
$\bar{t}_{S_C}$	shell thickness required to preclude compressive failure
$\bar{t}_{S_G}$	shell thickness required to meet minimum gage constraint
$\bar{t}_{S_T}$	shell thickness required to preclude tensile failure
$\bar{t}_T$	smeared tension tie thickness
$\bar{t}_w$	smeared wall thickness
$\bar{t}_{wG}$	thickness of wall to meet minimum gage constraint
$\bar{t}_{wT}$	thickness of wall required to prevent tensile failure
T	torque on wing carrythrough structure
VB	fuselage volume
V_W	volume of wing structural box, including structural components
V_1	volume of nose section of fuselage
V_2	volume of tail section of fuselage
w_C	width of carrythrough structure of wing
W	weight of aircraft structure
W'	weight of wing per unit span
W_B	weight of fuselage structure and attached components
W_{FT}	weight of fuel
W_I	ideal fuselage structural weight
W_{NO}	weight of nonoptimum material
W_S	vehicle longitudinal weight distribution
W_{TO}	gross takeoff weight of aircraft
W/S	shell structural weight per unit surface area
x	longitudinal fuselage coordinate
x_{calc}	weight calculated by PDCYL
x_{HT}	distance from nose to theoretical quarter chord of horizontal tail
x_{LE}	distance from nose to leading edge of wing at theoretical root chord
x_{P_1}	distance from nose to leading edge of fuselage mounted propulsion
x_{P_2}	distance from nose to trailing edge of fuselage mounted propulsion

y	transverse fuselage coordinate; wing coordinate measured along quarter chord
y_{act}	actual weight
y_{est}	estimated weight after regression
z	vertical fuselage coordinate
$Z(y)$	total width of wing box as a function of position along quarter chord
$Z_S(y)$	width of wing box structure as a function of position along quarter chord
δ	frame deflection
ε	shell buckling efficiency
ε_C	wing cover structural efficiency
ε_W	wing web structural efficiency
Λ	wing sweep
μ	wing loading
ρ	structural material density
ρ_B	gross fuselage density
ρ_F	frame structural material density
σ_S	allowable shear stress for wing
Σ	sum over fuselage or wing length; solidity of wing
ψ	truss core angle

Analytical Fuselage and Wing Weight Estimation of Transport Aircraft

MARK D. ARDEMA,* MARK C. CHAMBERS,* ANTHONY P. PATRON,* ANDREW S. HAHN,
HIROKAZU MIURA, AND MARK D. MOORE

Ames Research Center

Summary

A method of estimating the load-bearing fuselage weight and wing weight of transport aircraft based on fundamental structural principles has been developed. This method of weight estimation represents a compromise between the rapid assessment of component weight using empirical methods based on actual weights of existing aircraft, and detailed, but time-consuming, analysis using the finite element method. The method was applied to eight existing subsonic transports for validation and correlation. Integration of the resulting computer program, PDCYL, has been made into the weights-calculating module of the AirCraft SYNThesis (ACSYNT) computer program. ACSYNT has traditionally used only empirical weight estimation methods; PDCYL adds to ACSYNT a rapid, accurate means of assessing the fuselage and wing weights of unconventional aircraft. PDCYL also allows flexibility in the choice of structural concept, as well as a direct means of determining the impact of advanced materials on structural weight.

Using statistical analysis techniques, relations between the load-bearing fuselage and wing weights calculated by PDCYL and corresponding actual weights were determined. A User's Manual and two sample outputs, one for a typical transport and another for an advanced concept vehicle, are given in the appendices.

Introduction

A methodology based on fundamental structural principles has been developed to estimate the load-carrying weight of the fuselage and basic box weight of the wing for aircraft, and has been incorporated into the AirCraft SYNThesis program (ACSYNT). This weight routine is also available to run independently of ACSYNT, and is a modification of a collection of previously developed structural programs (refs. 1–4). The main subroutine called by ACSYNT is PDCYL. This study has concentrated on modern transport aircraft because of the detailed weight information available, allowing the weights output from PDCYL to be compared to actual structural weights. The detailed weight statements also allow *nonoptimum* factors to be computed which, when multiplied by the load-bearing structural weights calculated by PDCYL, will give good representative total structure weight estimates. These nonoptimum factors will be computed through a regression analysis of a group of eight transport aircraft.

PDCYL is able to model both skin-stringer-frame and composite sandwich shell fuselage and wing box constructions. Numerous modifications were made to PDCYL and its associated collection of subroutines. These modifications include the addition of detailed fuselage shell geometry calculations; optional integration of a cylindrical fuselage midsection between the nose and tail sections; addition of landing and bump maneuvers to the load cases sizing the fuselage; ability to introduce an elliptical spanwise lift load distribution on the wing; variation of wing thickness ratio from tip to root; ability to place landing gear on the wing to relieve spanwise bending loads; distribution of propulsion system components between wing and fuselage; and the determination of maximum wingtip deflection.

Brief Description of ACSYNT

The Aircraft Synthesis Computer program, ACSYNT, is an integrated design tool used in the modeling of advanced aircraft for conceptual design studies (ref. 5). ACSYNT development began at NASA Ames Research Center in the 1970s and continues to this day. The ACSYNT program is quite flexible and can model a wide range of aircraft configurations and sizes, from remotely piloted high altitude craft to the largest transport.

The ACSYNT program uses the following modules, not necessarily in this order: Geometry, Trajectory, Aerodynamics, Propulsion, Stability, Weights, Cost, Advanced Aerodynamic Methods, and Takeoff. An ACSYNT run would normally progress as follows: the Geometry module is called to define the aircraft shape and configuration; the Trajectory module then runs the vehicle through a specified mission; finally the Weight and Cost

*Santa Clara University, Santa Clara, California. Work of the first two authors was supported by NASA Ames Research Center Grant NCC2-5068.

modules are executed. To determine the performance of the vehicle at each mission point, the Trajectory module will call the Aerodynamics and Propulsion modules.

After the mission is completed, the calculated weight of the aircraft may be compared with the initial estimate and an iteration scheme run to converge upon the required aircraft weight. This process is necessarily iterative as the aircraft weight ACSYNT calculates is dependent upon the initial weight estimate.

ACSYNT is able to perform a *sensitivity analysis* on any design variable, such as aspect ratio, thickness-to-chord ratio, fuselage length or maximum fuselage diameter. Sensitivity is defined as (change in objective function/ value of objective function) divided by (change in design variable/design variable). As an example, if gross weight is the objective function and decreases when the wing thickness-to-chord ratio increases, then the sensitivity of thickness-to-chord ratio is negative. It is important to note that while this increase in thickness-to-chord ratio lowers the gross weight of the aircraft, it may also have a detrimental effect on aircraft performance.

ACSYNT is also able to size multiple design variables by optimizing the objective function. The objective function represents the interactions between design disciplines such as structures, aerodynamics and propulsion. The automated sizing of design variables during the optimization process is accomplished using the gradient method. Two types of constraints may be imposed during the optimization process. These are performance-based constraints such as runway length or maximum roll angle, and side constraints on design variables such as limitations on wing span or fuselage length. ACSYNT never violates constraints during the optimization process so that each iteration produces a valid aircraft.

Methods of Weight Estimation

Two methods are commonly available to estimate the load-bearing fuselage weight and wing box structure weight of aircraft. These methods, in increasing order of complexity and accuracy, are empirical regression and detailed finite element structural analysis. Each method has particular advantages and limitations which will be briefly discussed in the following sections. There is an additional method based on classical plate theory (CPT) which may be used to estimate the weight of the wing box structure.

Empirical– The empirical approach is the simplest weight estimation tool. It requires knowledge of fuselage and wing weights from a number of similar existing aircraft in addition to various key configuration parameters of these aircraft in order to produce a linear regression. This regression is a function of the configuration parameters of the existing aircraft and is then scaled to give an estimate of fuselage and wing weights for an aircraft under investigation. Obviously, the accuracy of this method is dependent upon the quality and quantity of data available for existing aircraft. Also, the accuracy of the estimation will depend on how closely the existing aircraft match the configuration and weight of the aircraft under investigation. All of the empirical regression functions currently in the ACSYNT program give total fuselage weight and total wing weight.

Finite Element– Finite element analysis is the matrix method of solution of a discretized model of a structure. This structure, such as an aircraft fuselage or wing, is modeled as a system of elements connected to adjacent elements at nodal points. An element is a discrete (or finite) structure that has a certain geometric makeup and set of physical characteristics. A nodal force acts at each nodal point, which is capable of displacement. A set of mathematical equations may be written for each element relating its nodal displacements to the corresponding nodal forces. For skeletal structures, such as those composed of rods or beams, the determination of element sizing and corresponding nodal positioning is relatively straightforward. Placement of nodal points on these simple structures would naturally fall on positions of concentrated external force application or joints, where discontinuities in local displacement occur.

Continuum structures, such as an aircraft fuselage or wing, which would use some combination of solid, flat plate, or shell elements, are not as easily discretizable. An approximate mesh of elements must be made to model these structures. In effect, an idealized model of the structure is made, where the element selection and sizing is tailored to local loading and stress conditions.

The assembly of elements representing the entire structure is a large set of simultaneous equations that, when combined with the loading condition and physical constraints, can be solved to find the unknown nodal forces and displacements. The nodal forces and displacements are then substituted back into the each element to produce stress and strain distributions for the entire structural model.

Classical Plate Theory– CPT has been applied to wing structure design and weight estimation for the past 20 years. Using CPT a mathematical model of the wing based on an equivalent plate representation is combined with global Ritz analysis techniques to study the structural response of the wing. An equivalent plate model does not require detailed structural design data as required for finite element analysis model generation and has been shown to be a reliable model for low aspect ratio fighter

wings. Generally, CPT will overestimate the stiffness of more flexible, higher aspect ratio wings, such as those employed on modern transport aircraft. Recently, transverse shear deformation has been included in equivalent plate models to account for this added flexibility. This new technique has been shown to give closer representations of tip deflection and natural frequencies of higher aspect ratio wings, although it still overestimates the wing stiffness. No fuselage weight estimation technique which corresponds to the equivalent plate model for wing structures is available.

Need for Better, Intermediate Method

Preliminary weight estimates of aircraft are traditionally made using empirical methods based on the weights of existing aircraft, as has been described. These methods, however, are undesirable for studies of unconventional aircraft concepts for two reasons. First, since the weight estimating formulas are based on existing aircraft, their application to unconventional configurations (i.e., canard aircraft or area ruled bodies) is suspect. Second, they provide no straightforward method to assess the impact of advanced technologies and materials (i.e., bonded construction and advanced composite laminates).

On the other hand, finite-element based methods of structural analysis, commonly used in aircraft detailed design, are not appropriate for conceptual design, as the idealized structural model must be built off-line. The solution of even a moderately complex model is also computationally intensive and will become a bottleneck in the vehicle synthesis. Two approaches which may simplify finite-element structural analysis also have drawbacks. The first approach is to create detailed analyses at a few critical locations on the fuselage and wing, then extrapolate the results to the entire aircraft, but this can be misleading because of the great variety of structural, load, and geometric characteristics in a typical design. The second method is to create an extremely coarse model of the aircraft, but this scheme may miss key loading and stress concentrations in addition to suffering from the problems associated with a number of detailed analyses.

The fuselage and wing structural weight estimation method employed in PDCYL is based on another approach, beam theory structural analysis. This results in a weight estimate that is directly driven by material properties, load conditions, and vehicle size and shape, and is not confined to an existing data base. Since the analysis is done station-by-station along the vehicle longitudinal axis, and along the wing structural chord, the distribution of loads and vehicle geometry is accounted for, giving an integrated weight that accounts for local conditions. An analysis based solely on fundamental principles will give an accurate estimate of structural weight only. Weights for fuselage and wing secondary structure, including control surfaces and leading and trailing edges, and some items from the primary structure, such as doublers, cutouts, and fasteners, must be estimated from correlation to existing aircraft.

The equivalent plate representation, which is unable to model the fuselage structure, is not used in PDCYL.

Methods

Overview

Since it is necessary in systems analysis studies to be able to rapidly evaluate a large number of specific designs, the methods employed in PDCYL are based on idealized vehicle models and simplified structural analysis. The analyses of the fuselage and wing structures are performed in different routines within PDCYL, and, as such, will be discussed separately. The PDCYL weight analysis program is initiated at the point where ACSYNT performs its fuselage weight calculation. PDCYL first performs a basic geometrical sizing of the aircraft in which the overall dimensions of the aircraft are determined and the propulsion system, landing gear, wing, and lifting surfaces are placed.

Fuselage– The detailed fuselage analysis starts with a calculation of vehicle loads on a station-by-station basis. Three types of loads are considered—longitudinal acceleration (applicable to high-thrust propulsion systems), tank or internal cabin pressure, and longitudinal bending moment. All of these loads occur simultaneously, representing a critical loading condition. For longitudinal acceleration, longitudinal stress resultants caused by acceleration are computed as a function of longitudinal fuselage station; these stress resultants are compressive ahead of the propulsion system and tensile behind the propulsion system. For internal pressure loads, the longitudinal distribution of longitudinal and circumferential (hoop) stress resultants is computed for a given shell gage pressure (generally 12 psig). There is an option to either use the pressure loads to reduce the compressive loads from other sources or not to do this; in either case, the pressure loads are added to the other tensile loads.

Longitudinal bending moment distributions from three load cases are examined for the fuselage. Loads on the fuselage are computed for a quasi-static pull-up maneuver, a landing maneuver, and travel over runway bumps. These three load cases occur at user-specified fractions of gross takeoff weight. Aerodynamic loads are computed as a constant fraction of fuselage planform area and are considered negligible for subsonic transports. For

pitch control there is an option to use either elevators mounted on the horizontal tail (the conventional configuration) or elevons mounted on the trailing edges of the wing. The envelope of maximum bending moments is computed for all three load cases and is then used to determine the net stress resultants at each fuselage station.

After the net stress resultants are determined at each fuselage station, a search is conducted at each station to determine the amount of structural material required to preclude failure in the most critical condition at the most critical point on the shell circumference. This critical point is assumed to be the outermost fiber at each station. Failure modes considered are tensile yield, compressive yield, local buckling, and gross buckling of the entire structure. A minimum gage restriction is also imposed as a final criterion. It is assumed that the material near the neutral fiber of the fuselage (with respect to longitudinal bending loads) is sufficient to resist the shear and torsion loads transmitted through the fuselage. For the shear loads this is a good approximation as the fibers farthest from the neutral axis will carry no shear. Also, for beams with large fineness ratios (fuselage length/maximum diameter) bending becomes the predominant failure mode.

The maximum stress failure theory is used for predicting yield failures. Buckling calculations assume stiffened shells behave as wide columns and sandwich shells behave as cylinders. The frames required for the stiffened shells are sized by the Shanley criterion. This criterion is based on the premise that, to a first-order approximation, the frames act as elastic supports for the wide column (ref. 6).

There are a variety of structural geometries available for the fuselage. There is a simply stiffened shell concept using longitudinal frames. There are three concepts with Z-stiffened shells and longitudinal frames; one with structural material proportioned to give minimum weight in buckling, one with buckling efficiency compromised to give lighter weight in minimum gage, and one a buckling-pressure compromise. Similarly, there are three truss-core sandwich designs, two for minimal weight in buckling with and without frames, and one a buckling-minimum gage compromise.

It is assumed that the structural materials exhibit elasto-plastic behavior. Further, to account for the effects of creep, fatigue, stress-corrosion, thermal cycling and thermal stresses, options are available to scale the material properties of strength and Young's modulus of elasticity. In the numerical results of this study, all materials were considered elastic and the full room-temperature material properties were used.

Composite materials can be modeled with PDCYL by assuming them to consist of orthotropic lamina formed into quasi-isotropic (two-dimensionally, or planar, isotropic) laminates. Each of the lamina is assumed to be composed of filaments placed unidirectionally in a matrix material. Such a laminate has been found to give very nearly minimum weight for typical aircraft structures.

Wing– The wing structure is a multi-web box beam designed by spanwise bending and shear. The wing-fuselage carrythrough structure, defined by the wing-fuselage intersection, carries the spanwise bending, shear, and torsion loads introduced by the outboard portion of the wing.

The load case used for the wing weight analysis is the quasi-static pull-up maneuver. The applied loads to the wing include the distributed lift and inertia forces, and the point loads of landing gear and propulsion, if placed on the wing. Fuel may also be stored in the wing, which will relieve bending loads during the pull-up maneuver.

The wing weight analysis proceeds in a similar fashion to that of the fuselage. The weight of the structural box is determined by calculating the minimum amount of material required to satisfy static buckling and strength requirements at a series of spanwise stations. The covers of the multi-web box are sized by buckling due to local instability and the webs by flexure-induced crushing. Required shear material is computed independently of buckling material. Aeroelastic effects are not accounted for directly, although an approximation of the magnitude of the tip deflection during the pull-up maneuver is made. For the carrythrough structure, buckling, shear, and torsion material are computed independently and summed.

As for the fuselage, there are a variety of structural geometries available. There are a total of six structural concepts, three with unstiffened covers and three with truss-stiffened covers. Both cover configurations use webs that are either Z-stiffened, unflanged, or trusses.

Geometry

Fuselage– The fuselage is assumed to be composed of a nose section, an optional cylindrical midsection, and a tail section. The gross density and fineness ratio are defined as

$$\rho_B = \frac{W_B}{V_B} \tag{1}$$

$$R_{fin} = \frac{l_B}{D} \tag{2}$$

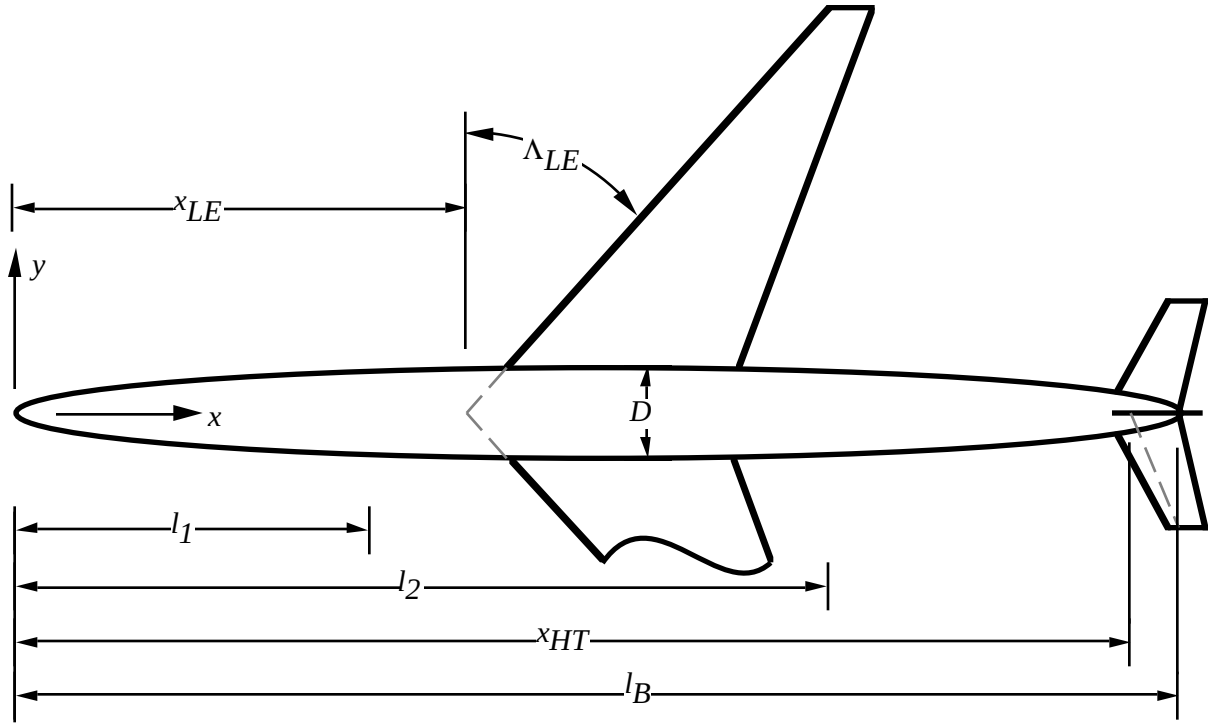

Figure 1. The body configuration.

where W_B is the fuselage weight (W_B = gross takeoff weight excluding the summed weight of the wing, tails, wing-mounted landing gear, wing-mounted propulsion, and fuel if stored in the wing), V_B is the total fuselage volume, l_B is the fuselage length, and D is the maximum fuselage diameter. The fuselage outline is defined by two power-law bodies of revolution placed back-to-back, with an optional cylindrical midsection between them (fig. 1). (For the present study, all eight transports used for validation of the analysis used the optional cylindrical midsection.)

With the cylindrical midsection, integration gives the fuselage volume, fuselage planform area, and fuselage surface area as

$$V_B = \frac{\pi D^2}{4}\left[\frac{l_1}{2P_1+1} + \left(l_B - l_2 - l_1\right) + \frac{l_2}{2P_2+1}\right] \tag{3}$$

$$S_B = D\left[\frac{l_1}{P_1+1} + \left(l_B - l_2 - l_1\right) + \frac{l_2}{P_2+1}\right] \tag{4}$$

$$A_B = \pi S_B \tag{5}$$

respectively, where l_1 and l_2 are the respective lengths to the start and end of the cylindrical midsection, and P_1 and P_2 are the respective powers that describe the nose and tail sections. P_1 and P_2, again for the case of the cylindrical midsection, are found by solving the power-law equations for the volumes of the nose and tail sections, which are input from ACSYNT. The solution of these equations gives the respective nose and tail powers as

$$P_1 = \frac{\pi D^2 l_1}{8V_1} - \frac{1}{2} \tag{6}$$

$$P_2 = \frac{\pi D^2 l_2}{8V_2} - \frac{1}{2} \tag{7}$$

where V_1 and V_2 are the corresponding nose and tail volumes.

The horizontal tail is placed according to its quarter chord location as a fraction of the fuselage length. The distance from the nose to the tail is

$$x_{HT} = l_B R_{HT} \tag{8}$$

where R_{HT} is the ratio of horizontal tail station to fuselage length.

Propulsion may be either mounted on the fuselage or placed on the wing. In the case of fuselage mounted propulsion, the starting and ending positions of the propulsion unit are again calculated from their respective fractions of fuselage length as

$$x_{P_1} = l_B R_{P_1} \tag{9}$$

$$x_{P_2} = l_B R_{P_2} \tag{10}$$

where R_{P1} and R_{P2} are the corresponding ratios of lengths to the leading and trailing edges of the fuselage engine pod to fuselage length.

Similarly, the nose landing gear is placed on the fuselage as a fraction of vehicle length; the main gear, on the other hand, may be placed either on the fuselage as a single unit, also as a fraction of fuselage length, or on the wing in multiple units as will be described below. The positions of the respective nose and optional fuselage-mounted main gear are

$$l_{NG} = l_B R_{NG} \tag{11}$$

$$l_{MG} = l_B R_{MG} \tag{12}$$

where R_{NG} and R_{MG} are the corresponding length ratios for the nose gear and main gear stations to vehicle length.

Wing– The lifting planforms are assumed to be tapered, swept wings with straight leading and trailing edges. The planform shape is trapezoidal as the root chord and tip chord are parallel.

The wing loading is defined as

$$\mu = \frac{W_{TO}}{S_P} \tag{13}$$

where S_P is the wing planform area.

The wing is placed on the fuselage according to the location of the leading edge of its root chord, determined as a fraction of the fuselage length. The distance from the nose to the leading edge of the wing is

$$x_{LE} = l_B R_{LE} \tag{14}$$

where R_{LE} is the ratio of leading edge station to fuselage length.

The first step in computing the wing weight is the determination of the geometry of the structural wing box. In terms of the input parameters W_{TO}, (W/S_p), aspect ratio (AR), taper ratio (R_{TAP}), and leading edge sweep (Λ_{LE}), the dependent parameters wing area, span, root chord, tip chord, and trailing edge wing sweep are computed from

$$S_P = \frac{W_{TO}}{W/S} \tag{15}$$

$$b = \sqrt{(AR)S_P} \tag{16}$$

$$C'_R = \frac{2S_P}{b(1+R_{TAP})} \tag{17}$$

$$C_T = R_{TAP} C'_R \tag{18}$$

$$\tan(\Lambda_{TE}) = \tan(\Lambda_{LE}) + \frac{2C'_R}{b}(R_{TAP} - 1) \tag{19}$$

(fig. 2). It is assumed that specified portions of the streamwise (aerodynamic) chord are required for controls and high lift devices, leaving the remainder for the structural wing box. The portions of the leading and trailing edges that are left for nonstructural use are specified as respective fractions C_{s_1} and $C_{s_2}$of the streamwise chord. Determination of these chord fractions is accomplished through visual inspection of the wing planform. Measured at the theoretical root chord, the dimensions for the leading and trailing edges are

$$l_{LE} = C_{S_1} C'_R \tag{20}$$

$$l_{TE} = C_{S_2} C'_R \tag{21}$$

respectively. The intersection of this structural box with the fuselage contours determines the location of the rectangular carrythrough structure. The width of the carrythrough structure, w_C, is defined by the corresponding fuselage diameter.

The dimensions of the structural box and of the carrythrough structure are now determined (fig. 3). The structural semispan, b_S, is assumed to lie on the quarter-chord line, y, whose sweep is given by

$$\tan(\Lambda_S) = \frac{3}{4}\tan(\Lambda_{LE}) + \frac{1}{4}\tan(\Lambda_{TE}) \tag{22}$$

Thus,

$$b_S = \frac{b - D}{2\cos(\Lambda_S)} \tag{23}$$

The streamwise chord at any point on the wing is given by

$$r(\zeta) = C'_R - \frac{\zeta}{b/2}(C'_R - C_T) \tag{24}$$

where ζ is measured perpendicular to the vehicle longitudinal axis from the vehicle centerline toward the wingtip. Thus, the streamwise chord is the dimension of the wing parallel to the vehicle longitudinal axis. In particular, at the wing-fuselage intersection,

$$C_R = C'_R - \frac{D}{b}(C'_R - C_T) \tag{25}$$

The structural root and tip chords are

$$C_{SR} = (1 - C_{S_1} - C_{S_2})C_R \tag{26}$$

$$C_{ST} = (1 - C_{S_1} - C_{S_2})C_T \tag{27}$$

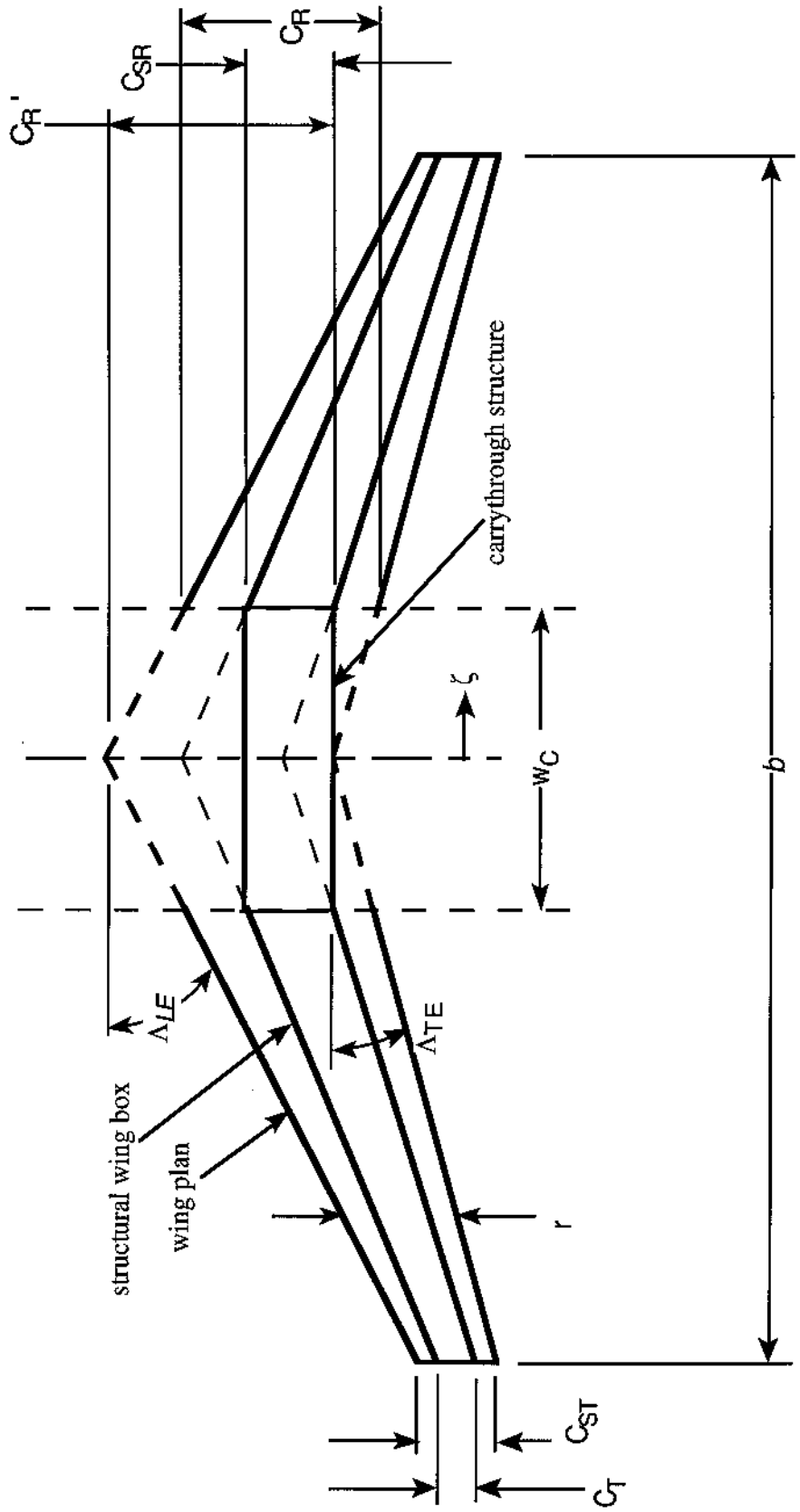

Figure 2. Wing structural planform geometry.

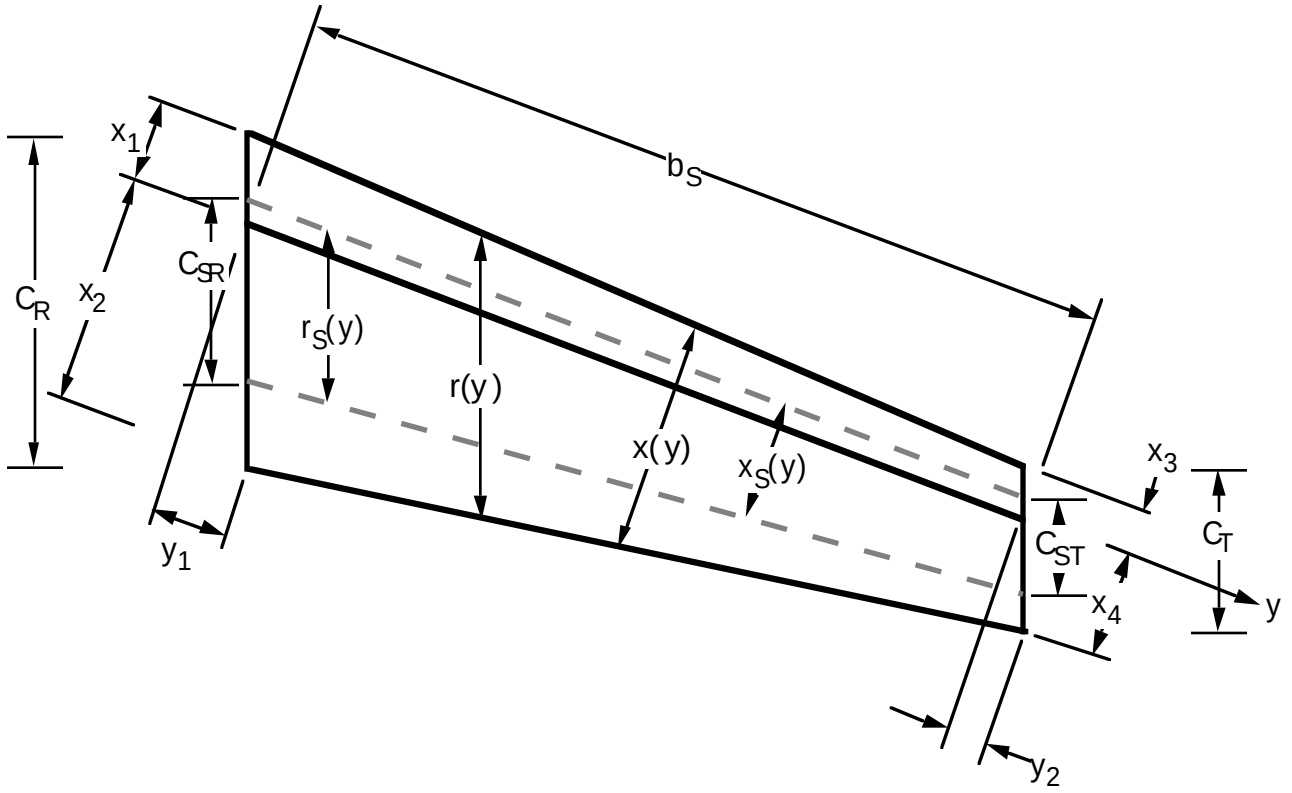

Figure 3. Wing coordinate system.

respectively. In terms of y, measured along the quarter chord from the wing-fuselage intersection toward the wingtip, the structural and total chords are given by

$$r_S(y) = C_{SR} - \frac{y}{b_S}\left(C_{SR} - C_{ST}\right) \tag{28}$$

$$r(y) = C_R - \frac{y}{b_S}\left(C_R - C_T\right) \tag{29}$$

where the structural chord is defined as the dimension of the rectangular-section wing box measured parallel to the vehicle longitudinal axis. Computation of the widths of the wing box and total wing structure, as shown in figure 3, is relatively complicated due to the geometry at the wingtip and the wing-fuselage intersection. For the portion of the wing between the wingtip and the wing-fuselage intersection, the respective widths of the wing box and total wing structure at any spanwise station y are

$$Z_S(y) = r_S \cos\left(\Lambda_S\right) \tag{30}$$

$$Z(y) = r \cos\left(\Lambda_S\right) \tag{31}$$

where $Z_S(y)$ and $Z(y)$ are dimensions perpendicular to the structural semispan.

The thickness of the wing box at any spanwise station y is determined as a linear interpolation between the root and tip thickness ratios multiplied by the chord at y.

$$t(y) = \begin{Bmatrix} rR_t(y), & 0 \le y \le b_S \quad \text{(box structure)} \\ rR_t(0), & y < 0 \quad \text{(carrythrough structure)} \end{Bmatrix} \tag{32}$$

where $R_t(y)$ is the thickness ratio of the wing as a function of position along the quarter chord.

For the transports in the present study, all the fuel is carried within the wing structure. An option is also available to carry the fuel entirely within the fuselage, negating any bending relief in the wing. (The high altitude drone, described in Appendix B, was modeled with a fuselage fuel tank.) The volume of the trapezoidal planform, rectangular-section wing box structure (including the carrythrough structure) is found as follows:

$$
\begin{aligned}
V_W &= 2\int_0^{b_S} Z_S(y)t(y)dy + \left(1 - C_{S_1} - C_{S_2}\right)R_{t_R}C_R^2 w_C \\
&= 2\cos(\Lambda_S)\left(1 - C_{S_1} - C_{S_2}\right) \\
&\quad \times \int_0^{b_S}\left[C_R - \frac{y}{b_S}\left(C_R - C_T\right)\right] \\
&\quad \times \left[R_{t_R}C_R - \frac{y}{b_S}\left(R_{t_R}C_R - R_{t_T}C_T\right)\right]dy \\
&\quad + \left(1 - C_{S_1} - C_{S_2}\right)R_{t_R}C_R^2 w_C \\
&= \frac{b_S\left(1 - C_{S_1} - C_{S_2}\right)\cos(\Lambda_S)}{3} \\
&\quad \times \left[R_{t_R}C_R\left(2C_R + C_T\right) + R_{t_T}C_T\left(C_R + 2C_T\right)\right] \\
&\quad + \left(1 - C_{S_1} - C_{S_2}\right)R_{t_R}C_R^2 w_C
\end{aligned}
\tag{33}
$$

This equation is based on flat upper and lower surfaces and neglects the volume taken up by the structure.

Loads

Fuselage– Fuselage loading is determined on a station-by-station basis along the length of the vehicle. Three types of fuselage loads are considered—longitudinal acceleration, tank pressure, and bending moment. In the present study, all three load types are assumed to occur simultaneously to determine maximum compressive and tensile loads at the outer shell fibers at each station.

Bending loads applied to the vehicle fuselage are obtained by simulating vehicle pitch-plane motion during a quasi-static pull-up maneuver; a landing; and movement over a runway bump. Simplified vehicle loading models are used where it is assumed that: (1) fuselage lift forces (nominally zero for subsonic transports) are distributed uniformly over the fuselage plan area; (2) wing loading, determined independently, is transferred by a couple of vertical force and torque through the wing carrythrough structure; (3) fuselage weight is distributed uniformly over fuselage volume; (4) control surface forces and landing gear reactions are point loads; and (5) the propulsion system weight, if mounted on the fuselage, is uniformly distributed. A factor of safety (nominally 1.5) is applied to each load case. The aircraft weight for each case is selected as a fraction of gross takeoff weight. The resulting one-dimensional loading model is shown in figure 4. All fuselage lift forces are assumed to be linear functions of angle of attack. Longitudinal bending moments are computed for each of the three loading cases and the envelope of the maximum values taken as the design loading condition. The bending moment computation is given in detail in reference 4 and will only be summarized here.

Considering first the pull-up maneuver loading, the motion is assumed to be a quasi-static pitch-plane pull-up of given normal load factor *n* (nominally 2.5 for transport aircraft). The vehicle is trimmed with the appropriate control surface (a horizontal tail for all eight transport used for validation in the present study), after which the angle of attack is calculated.

Landing loads are developed as the aircraft descends at a given vertical speed, V_S, after which it impacts the ground; thereafter the main and nose landing gears are assumed to exert a constant, or optionally a $(1 - \cos(\omega t))$, force during its stroke, S_{LG}, until the aircraft comes to rest. The vehicle weight is set equal to the nominal landing weight. Wing lift as a fraction of landing weight is specified, which reduces the effective load the landing gear carries. Likewise, the portion of total vehicle load the main gear carries is specified. No pitch-plane motion is considered during the landing.

Runway bump loads are handled by inputting the bump load factor into the landing gear. Bump load factor is applied according to reference 7. This simulates the vehicle running over a bump during taxi. In a similar fashion to the landing, the wing lift as a fraction of gross takeoff weight is specified, as is the portion of effective load input through the main gear. No pitch-plane motion is considered during the bump.

Wing– For the wing, only a quasi-static pull-up maneuver condition at load factor *n* is considered for determining loads. At each spanwise station along the quarter chord, from the wingtip to the wing-fuselage intersection, the lift load, center of pressure, inertia load, center of gravity, shear force, and bending moment are computed. For the inertia load, it is assumed that the fuel weight W_{FT} is distributed uniformly with respect to the wing volume so that the inertial load at y is $(W_{FT}/V_W)*V(y)$, where $V(y)$ is the volume outboard of y; this volume has centroid $C_g(y)$ with respect to station y. An estimate of the wing structural weight is included in W_{FT} for this calculation but the calculation is not redone when the actual structural weight has been computed.

There is an option for either a trapezoidal or a Schrenk (ref. 8) lift load distribution along the wingspan; the trapezoidal distribution represents a uniform lift over the wing area (which has a trapezoidal planform) while the

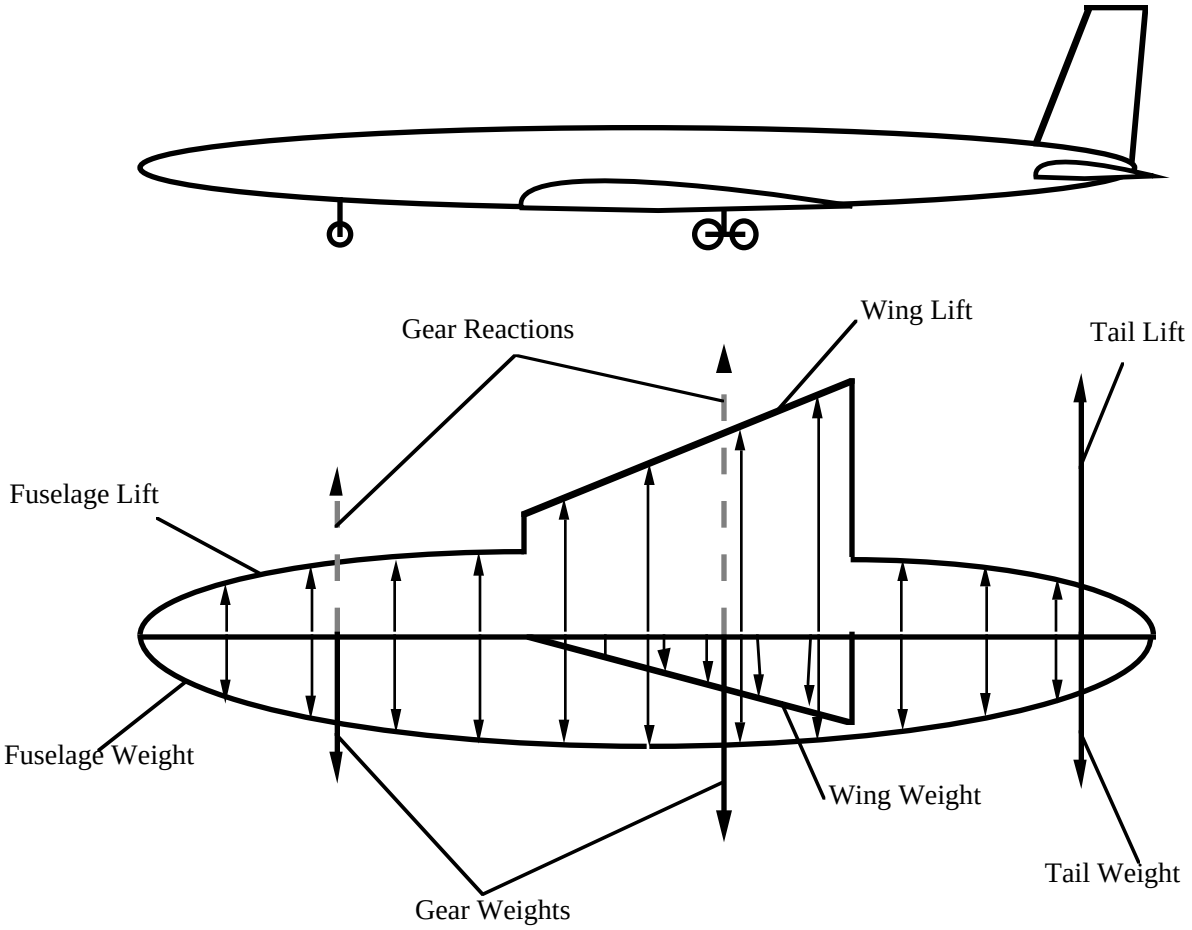

Figure 4. Loading model.

Schrenk distribution is an average of the trapezoidal distribution with an elliptical distribution, where the lift is zero at the wingtip and maximum at the wing-fuselage intersection. Prandtl has shown that a true elliptical lift load distribution will have a minimum induced drag, but a combination of the elliptical and trapezoidal distributions will give a better representation of actual aircraft loading (ref. 8).

Plots of trapezoidal and Schrenk lift load distributions are shown in figure 5. For the trapezoidal lift load distribution the lift load at y is $(W/S)A_{TRAP}(y)$, where $A_{TRAP}(y)$ is the area outboard of y; the centroid of this area is denoted $C_{P_{TRAP}}(y)$, where y is measured along the quarter chord. For the elliptical lift load distribution, the lift load matches the contour of an ellipse with the end of its major axis on the tip and the end of its minor axis directly above the wing-fuselage intersection. The area enclosed by the quadrant of the ellipse is set equal to the exposed area of the trapezoidal wing panel

$$S_{ELL} = \frac{(b - w_C)}{4}(1 + R_{TAP})C_R \tag{34}$$

Thus the value of lift at y, L_{ELL}, the area of ellipse outboard of y, A_{ELL}, and the center of pressure of lift outboard of y, $C_{P_{ELL}}$, for y measured along the structural box may be determined as

$$L_{ELL}(y) = \frac{4S_{ELL}}{\pi b_S}\left[1 - \left(\frac{y}{b_S}\right)^2\right]^{\frac{1}{2}} \tag{35}$$

$$A_{ELL}(y) = S_{ELL} - \left\{\frac{2S_{ELL}}{\pi {b_S}^2}\left[y\left({b_S}^2 - y^2\right)^{\frac{1}{2}} + {b_S}^2 \sin^{-1}\left(\frac{y}{b_S}\right)\right]\right\} \tag{36}$$

$$C_{P_{ELL}}(y) = \frac{4}{3\pi}(b_S - y) \tag{37}$$

respectively.

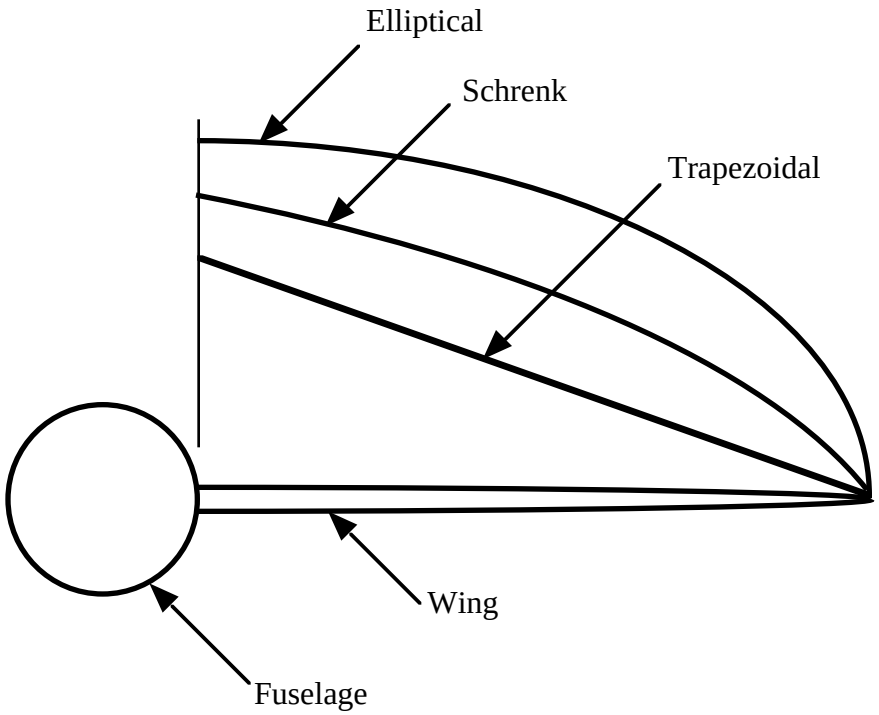

Figure 5. Trapezoidal and Schrenk lift load distributions.

For the Schrenk lift load distribution, the average of $A_{TRAP}(y)$ and $A_{ELL}(y)$ is used to represent the composite area, while the average of $C_{P_{TRAP}}(y)$ and $C_{P_{ELL}}(y)$ is used to represent the composite center of pressure.

Using the appropriate outboard area $A(y)$ and center of pressure $C_P(y)$, the shear force is

$$F_S(y) = nK_S\left[\frac{W}{S}A - \frac{W_{FT}}{V_W}V - \sum_{i=1}^{n_e} h_e\left(y_{e_i} - y\right)W_{e_i} - \sum_{i=1}^{n_{lg}} h_{lg}\left(y_{lg_i} - y\right)W_{lg_i}\right] \tag{38}$$

where n_e and n_{lg} are the number of engines and landing gear mounted on the semispan, respectively; W_{e_i} and W_{lg_i} are the weights of the i^{th} engine an i^{th} landing gear, respectively; y_{e_i} and y_{lg_i} are the locations of the i^{th} engine and i^{th} landing gear, respectively; and

$$h_e\left(y_{e_i} - y\right) = \begin{Bmatrix} 1, & y_{e_i} > y \\ 0, & y_{e_i} < y \end{Bmatrix} \tag{39}$$

$$h_{lg}\left(y_{lg_i} - y\right) = \begin{Bmatrix} 1, & y_{lg_i} > y \\ 0, & y_{lg_i} < y \end{Bmatrix} \tag{40}$$

The bending moment is

$$M(y) = nK_S\left[\frac{W}{S}AC_P - \frac{W_{FT}}{V_W}VC_g - \sum_{i=1}^{n_e} h_e\left(y_{e_i} - y\right)W_{e_i}\left(y_{e_i} - y\right) - \sum_{i=1}^{n_{lg}} h_{lg}\left(y_{lg_i} - y\right)W_{lg_i}\left(y_{lg_i} - y\right)\right] \tag{41}$$

Structural Analysis

Fuselage– Weight estimating relationships are now developed for the load-carrying fuselage structure. In addition, the volume taken up by the fuselage structure is also determined.

Considering first the circular shell, the stress resultants in the axial direction caused by longitudinal bending, axial acceleration, and pressure at a fuselage station x are

$$N_{x_B} = \frac{Mr}{I'_y} \tag{42}$$

$$N_{x_A} = \frac{N_x W_S}{P} \tag{43}$$

$$N_{x_P} = \frac{AP_g}{P} \tag{44}$$

respectively, where $r = D/2$ is the fuselage radius, $A = \pi r^2$ is the fuselage cross-sectional area, and $P = 2\pi r$ is the fuselage perimeter. In equation 42, $I'_y = \pi r^3$ is the moment of inertia of the shell divided by the shell thickness. In equation 43, for the case of fuselage-mounted propulsion, W_S is the portion of vehicle weight ahead of station x if x is ahead of the inlet entrance, or the portion of vehicle weight behind x if x is behind the nozzle exit. In equation 44, P_g is the limit gage pressure differential for the passenger compartment during cruise. The total tension stress resultant is then

$$N_x^+ = N_{x_B} + N_{x_P} \tag{45}$$

if x is ahead of the nozzle exit, and

$$N_x^+ = N_{x_B} + N_{x_P} + N_{x_A} \tag{46}$$

if x is behind it. Similarly, the total compressive stress resultant is

$$N_x^- = N_{x_B} + N_{x_A} - \begin{Bmatrix} 0, & \text{if not pressure stabilized} \\ N_{x_P}, & \text{if stabilized} \end{Bmatrix} \tag{47}$$

if x is ahead of the inlet entrance, and

$$N_x^- = N_{x_B} - \begin{Bmatrix} 0, & \text{if not pressure stabilized} \\ N_{x_P}, & \text{if stabilized} \end{Bmatrix} \tag{48}$$

if x is behind it. These relations are based on the premise that acceleration loads never decrease stress resultants, but pressure loads may relieve stress, if pressure stabilization is chosen as an option. The stress resultant in the hoop direction is

$$N_y = rP_g K_P \tag{49}$$

where K_p accounts for the fact that not all of the shell material (for example, the core material in sandwich designs) is available for resisting hoop stress.

The equivalent isotropic thicknesses of the shell are given by

$$\bar{t}_{S_C} = \frac{N_x^-}{F_{cy}} \tag{50}$$

$$\bar{t}_{S_T} = \frac{1}{F_{tu}} \max\left(N_x^+, N_y\right) \tag{51}$$

$$\bar{t}_{S_G} = K_{mg} t_{mg} \tag{52}$$

for designs limited by compressive yield strength (F_{cy}), ultimate tensile strength (F_{tu}), and minimum gage, respectively. In equation 52, t_{mg} is a specified minimum material thickness and K_{mg} is a parameter relating $\bar{t}_{S_G}$ to t_{mg} which depends on the shell geometry.

A fourth thickness that must be considered is that for buckling critical designs, $\bar{t}_{S_B}$, which will now be developed. The nominal vehicles of this study have integrally stiffened shells stabilized by ring frames. In the buckling analysis of these structures, the shell is analyzed as a wide column and the frames are sized by the Shanley criteria (ref. 6). Expressions are derived for the equivalent isotropic thickness of the shell required to preclude buckling, $\bar{t}_{S_B}$, and for the *smeared* equivalent isotropic thickness of the ring frames required to preclude general instability, $\bar{t}_F$. The analysis will be restricted to the case of cylindrical shells. The major assumptions are that the structural shell behaves as an Euler beam and that all structural materials behave elastically.

For the stiffened shell with frames concept, the common procedure of assuming the shell to be a wide column is adopted. If the frame spacing is defined as d and Young's modulus of the shell material is defined as E, the buckling equation is then

$$\frac{N_x^-}{dE} = \varepsilon\left(\frac{\bar{t}_{S_B}}{d}\right)^2 \tag{53}$$

or, solving for $\bar{t}_{S_B}$

$$\bar{t}_{S_B} = \sqrt{\frac{N_x^- d}{E\varepsilon}} \tag{54}$$

Fuselage structural geometry concepts are presented in table 1; values of the shell efficiency ε for the various structural concepts are given in table 2. The structural shell geometries available are simply stiffened, Z-stiffened, and truss-core sandwich. We next size the frames to prevent general instability failure. The Shanley criterion is based on the premise that the frames act as elastic supports for the wide column; this criterion gives the smeared equivalent thickness of the frames as

Table 1. Fuselage structural geometry concepts

KCON sets concept number	
2	Simply stiffened shell, frames, sized for minimum weight in buckling
3	Z-stiffened shell, frames, best buckling
4	Z-stiffened shell, frames, buckling-minimum gage compromise
5	Z-stiffened shell, frames, buckling-pressure compromise
6	Truss-core sandwich, frames, bestis, no frames, best buckling
9	Truss-core sandwich, no frames, buckling-minimum gage-pressure compromise

Table 2. Fuselage structural geometry parameters

Structural concept (KCON)	m	ε	K_{mg}	K_p	K_{th}
2	2	0.656	2.463	2.463	0.0
3	2	0.911	2.475	2.475	0.0
4	2	0.760	2.039	1.835	0.0
5	2	0.760	2.628	1.576	0.0
6	2	0.605	4.310	3.965	0.459
8	1.667	0.4423	4.820	3.132	0.405
9	1.667	0.3615	3.413	3.413	0.320

$$\bar{t}_{F_B} = 2r^2 \sqrt{\frac{\pi C_F N_x^-}{K_{F1} d^3 E_F}} \tag{55}$$

where C_F is Shanley's constant, K_{F1} is a frame geometry parameter, and E_F is Young's modulus for the frame material. (See ref. 3 for a discussion of the applicability of this criterion and for a detailed derivation of the equations presented here.) If the structure is buckling critical, the total thickness is

$$\bar{t} = \bar{t}_{S_B} + \bar{t}_{F_B} \tag{56}$$

Minimizing $\bar{t}$ with respect to d results in

$$\bar{t} = \frac{4}{27^{1/4}} \left(\frac{\pi C_F}{K_{F1} \varepsilon^3 E_F E^3} \right)^{\frac{1}{8}} \left(\frac{2r^2 \rho_F \left(N_x^- \right)^2}{\rho} \right)^{\frac{1}{4}} \tag{57}$$

$$\bar{t}_{S_B} = \frac{3}{4} \bar{t} \tag{58}$$

$$\bar{t}_{F_B} = \frac{1}{4} \bar{t} \tag{59}$$

$$d = \left(6r^2 \frac{\rho_F}{\rho} \sqrt{\frac{\pi C_F \varepsilon E}{K_{F1} E_F}} \right)^{\frac{1}{2}} \tag{60}$$

where ρ_F is the density of the frame material and ρ is the density of the shell material, so that the shell is three times as heavy as the frames.

Frameless sandwich shell concepts may also be used. For these concepts, it is assumed that the elliptical shell buckles at the load determined by the maximum compressive stress resultant N_x^- on the cylinder. The buckling equation for these frameless sandwich shell concepts is

$$\frac{N_x^-}{rE} = \varepsilon \left(\frac{\bar{t}_{S_B}}{r} \right)^m \tag{61}$$

where m is the buckling equation exponent. Or, solving for $\bar{t}_{S_B}$

$$\bar{t}_{S_B} = r\left(\frac{N_x^-}{rE\varepsilon}\right)^{\frac{1}{m}} \tag{62}$$

This equation is based on small deflection theory, which seems reasonable for sandwich cylindrical shells, although it is known to be inaccurate for monocoque cylinders. Values of m and ε may be found, for example in references 9 and 10 for many shell geometries. Table 2 gives values for sandwich structural concepts available in PDCYL, numbers 8 and 9, both of which are truss-core sandwich. The quantities N_x^-, r, and consequently $\bar{t}_{S_B}$, will vary with fuselage station dimension x.

At each fuselage station x, the shell must satisfy all failure criteria and meet all geometric constraints. Thus, the shell thickness is selected according to compression, tension, minimum gage, and buckling criteria, or

$$\bar{t}_S = \max\left(\bar{t}_{S_C}, \bar{t}_{S_T}, \bar{t}_{S_G}, \bar{t}_{S_B}\right) \tag{63}$$

If $\bar{t}_S = \bar{t}_{S_B}$, the structure is buckling critical and the equivalent isotropic thickness of the frames, $\bar{t}_F$, is computed from equation 59. If $\bar{t}_S > \bar{t}_{S_B}$, the structure is not buckling critical at the optimum frame sizing and the frames are resized to make $\bar{t}_S = \bar{t}_{S_B}$. Specifically, a new frame spacing is computed from equation 54 as

$$d = \frac{E\varepsilon\bar{t}_S^{\,2}}{N_x^-} \tag{64}$$

and this value is used in equation 55 to determine $\bar{t}_F$.

The total thickness of the fuselage structure is then given by the summation of the smeared weights of the shell and the frames

$$\bar{t}_B = \bar{t}_S + \bar{t}_F \tag{65}$$

The shell gage thickness may be computed from $\bar{t}_g = \bar{t}_S / K_{mg}$. The *ideal* fuselage structural weight is obtained by summation over the vehicle length

$$W_I = 2\pi\sum\left(\rho\bar{t}_{S_i} + \rho_F\bar{t}_{F_i}\right)r_i\Delta x_i \tag{66}$$

where the quantities subscripted i depend on x.

We next discuss the derivation of the structural geometry parameters shown in table 2. The Z-stiffened shell, typical of modern transport aircraft, will be used as an example of skin-stringer-frame construction. Using reference 9 and figure 6, the equivalent isotropic thickness of the smeared skin and stringers is

$$\bar{t}_S = t_s + \frac{2b_f f_f}{b_s} + \frac{b_w t_w}{b_s} = \left[1 + 1.6\left(\frac{b_w}{b_s}\right)\left(\frac{t_w}{t_s}\right)\right]t_s \tag{67}$$

Since only the skin is available for resisting pressure loads,

$$K_p = 1 + 1.6\left(\frac{b_w}{b_s}\right)\left(\frac{t_w}{t_w}\right) \tag{68}$$

For minimum gage designs, if $t_s > t_w$ then $t_w = t_{mg}$ and

$$\bar{t}_S = \left[\left(\frac{t_s}{t_w}\right) + 1.6\left(\frac{b_w}{b_s}\right)\right]t_{mg} \tag{69}$$

so that

$$K_{mg} = \left(\frac{t_s}{t_w}\right) + 1.6\left(\frac{b_w}{b_s}\right) \tag{70}$$

On the other hand, if $t^s < t^w$ then $t_s = t_{mg}$ and

$$\bar{t}_S = \left[1 + 1.6\left(\frac{b_w}{b_s}\right)\left(\frac{t_w}{t_s}\right)\right]t_{mg} \tag{71}$$

so that

$$K_{mg} = 1 + 1.6\left(\frac{b_w}{b_s}\right)\left(\frac{t_w}{t_s}\right) \tag{72}$$

Equations 68, 70, and 72 show that for both pressure loading critical and minimum gage limited structure, (b_w/b_s) and (t_w/t_s) should be as small as possible (i.e., no stringers). As an option in PDCYL, all of the detailed shell dimensions shown in figure 6 are computed and output at each fuselage station.

In practice, a typical design will be influenced by bending and pressure loads and by the minimum gage constraint, and thus a compromise is necessary. If buckling is of paramount importance, then a good choice is $(b_w/b_s) = 0.87$ and $(t_w/t_s) = 1.06$ because this gives the maximum buckling efficiency for this concept, namely $\varepsilon = 0.911$ (ref. 9). From equations 68 and 72,

$$K_p = K_{mg} = 1 + (1.6)(0.87)(1.06) = 2.475 \tag{73}$$

This is concept 3 in tables 1 and 2. If pressure dominates the loading condition, then $(b_w/b_s) = 0.6$ and $(t_w/t_s)=0.6$ is a reasonable choice, giving $\varepsilon = 0.76$, $K_p = 1.576$, and $K_{mg} = 2.628$; this is concept 5. For minimum gage dominated structure, the geometry $(b_w/b_s) = 0.58$ and $(t_w/t_s) = 0.90$ gives concept 6.

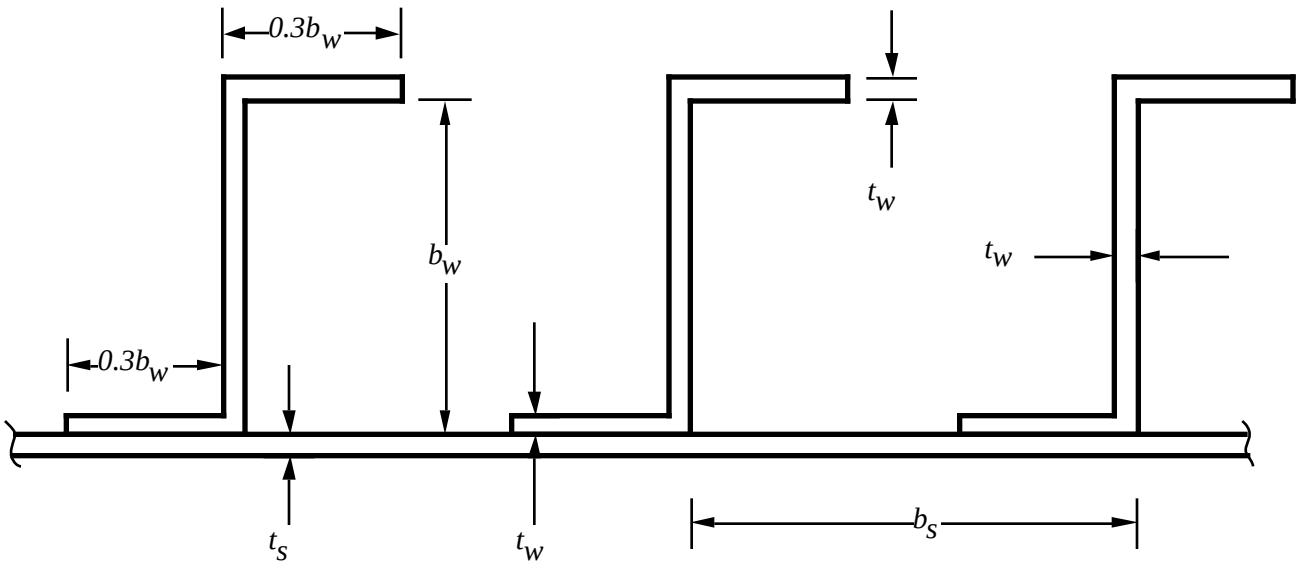

Figure 6. Typical Z-stiffened shell geometry.

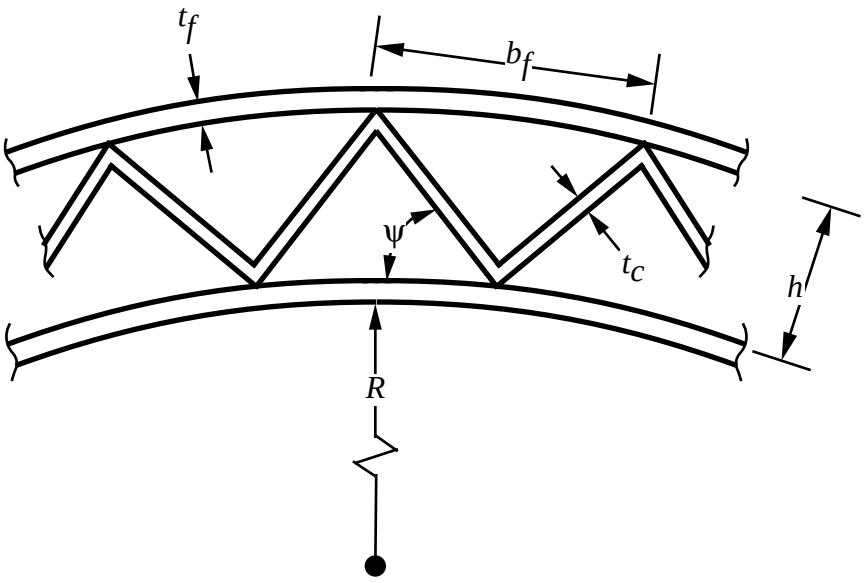

Figure 7. Truss-core sandwich geometry.

The geometry of the truss-core sandwich shell concept is shown in figure 7. The equivalent isotropic shell thickness of this concept is

$$\bar{t}_S = \left(2 + \frac{t_c}{t_f} \frac{1}{\cos(\psi)} \right) t_f \qquad (74)$$

Reference 9 shows that the optimum buckling efficiency is obtained for $(t_c/t_f) = 0.65$ and $\psi = 55$ deg. This gives $\varepsilon = 0.4423$, $K_{mg} = 4.820$, and $K_p = 3.132$, concept 8 in tables 1 and 2. To get a design that is lighter for minimum gage dominant structure, a geometry is chosen that places equal thickness material in the face sheets and the core; the choice of $(t_c/t_f) = 1.0$ and $\psi = 45$ deg gives structural concept 9. These calculations assume that the face sheets and core are composed of the same material and are subject to the same minimum gage constraint.

Since the preceding analysis gives only the ideal weight, W_I, the *nonoptimum* weight, W_{NO} (including fasteners, cutouts, surface attachments, uniform gage penalties, manufacturing constraints, etc.) has yet to be determined. The method used will be explained in a later section.

Wing– Using the geometry and loads applied to the wing developed above, the structural dimensions and weight of the structural box may now be calculated. The wing structure is assumed to be a rectangular multi-web box beam with the webs running in the direction of the structural semispan. Reference 9 indicates that the critical instability mode for multi-web box beams is simultaneous buckling of the covers due to local instability and of the webs due to flexure induced crushing. This reference gives the solidity (ratio of volume of structural material to total wing box volume) of the least weight multi-web box beams as

$$\Sigma = \varepsilon\left(\frac{M}{Z_S t^2 E}\right)^e \tag{75}$$

where ε and e depend on the cover and web geometries (table 3), M is the applied moment, t is the thickness, E is the elastic modulus, and Z_S is obtained from reference 9. The solidity is therefore

$$\Sigma = \frac{W'_{BEND}(y)}{\rho Z_S t} \tag{76}$$

where W'_{BEND} is the weight of bending material per unit span and ρ is the material density. W'_{BEND} is computed from equations 75 and 76. The weight per unit span of the shear material is

$$W'_{SHEAR}(y) = \frac{\rho F_S}{\sigma_S} \tag{77}$$

where F_S is the applied shear load and σ_S is the allowable shear stress. The optimum web spacing (fig. 8) is computed from (ref. 2)

$$d_W = t\left[\frac{(1-2e_C)}{(1-e_C)\sqrt{2\varepsilon_W}}\left(\frac{M}{Z_S t^2 E}\right)^{\frac{2e_C-3}{2e_C}} \varepsilon_C^{\frac{3}{2e_C}}\right]^{\frac{2e_C}{4e_C-3}} \tag{78}$$

where subscripts W and C refer to webs and covers, respectively. The equivalent isotropic thicknesses of the covers and webs are

$$\bar{t}_C - d_W\left(\frac{M}{Z_S t E \varepsilon_C d_W}\right)^{\frac{1}{e_C}} \tag{79}$$

$$\bar{t}_W = t\sqrt{\left(\frac{M}{Z_S t^2 E}\right)^{\left(2-\frac{1}{e_C}\right)}\left(\frac{\varepsilon_C d_W}{t}\right)^{\frac{1}{e_C}}\left(\frac{2}{\varepsilon_W}\right)} \tag{80}$$

respectively, and the gage thicknesses are

$$t_{g_C} = K_{g_C}\bar{t}_C \tag{81}$$

$$t_{g_W} = K_{g_W}\bar{t}_W \tag{82}$$

Values of ε, e, ε_C, E_C, ε_W, K_{g_w}, and K_{g_c} are found in table 3 for various structural concepts (ref. 9). If the wing structural semispan is divided into N equal length segments, the total *ideal* weight of the wing box structure is

$$W_{BOX} = \frac{2b_S}{N}\sum_{i=1}^{N}\left(W'_{BEND_i} + W'_{SHEAR_i}\right) \tag{83}$$

Table 3. Wing structural coefficients and exponents

Covers	Webs	ε	e	ε	e_c	ε_w	K_{g_c}	K_{g_w}
Unstiffened	Truss	2.25	0.556	3.62	3	0.605	1.000	0.407
Unstiffened	Unflanged	2.21	0.556	3.62	3	0.656	1.000	0.505
Unstiffened	Z-stiffened	2.05	0.556	3.62	3	0.911	1.000	0.405
Truss	Truss	2.44	0.600	1.108	2	0.605	0.546	0.407
Truss	Unflanged	2.40	0.600	1.108	2	0.656	0.546	0.505
Truss	Z-stiffened	2.25	0.600	1.108	2	0.911	0.546	0.405

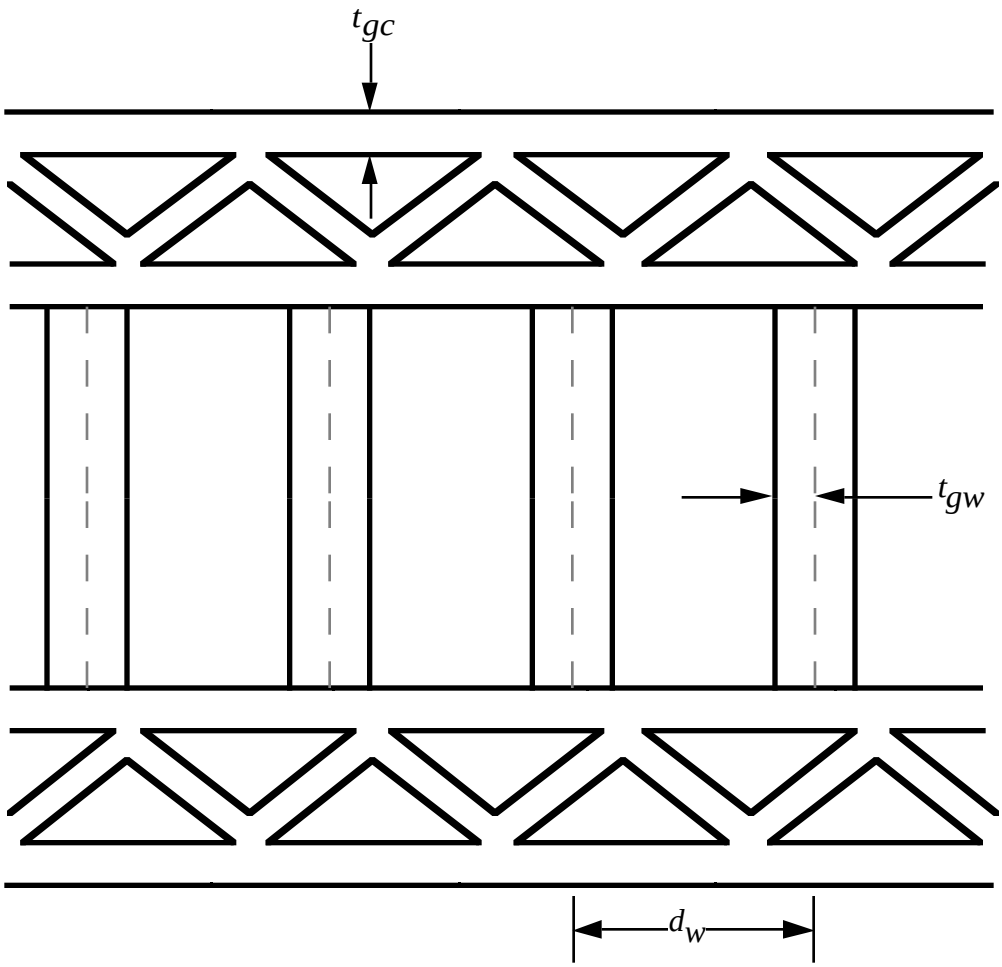

Figure 8. Wing structural concept.

The wing carrythrough structure consists of torsion material in addition to bending and shear material. The torsion material is required to resist the twist induced due to the sweep of the wing. The bending material is computed in a similar manner as that of the box except that only the longitudinal component of the bending moment contributes. Letting $t_0 = t(y = 0)$ and $M_0 = M(y = 0)$,

$$\Sigma_C = \varepsilon \left(\frac{M_0 \cos(\Lambda_S)}{t_0^2 C_{SR} E} \right)^e \tag{84}$$

The weight of the bending material is then

$$W_{BEND_C} = \rho \Sigma_C C_{SR} t_0 w_C \tag{85}$$

where w_C is the width of the carrythrough structure. (When the wing-fuselage intersection occurs entirely within the cylindrical midsection, as is the case with all eight transport used for validation in the present study, $w_C = D$.) The quantities d_W, t_W, and t_C are computed in the same manner as for the box. The weight of the shear material is

$$W_{SHEAR_C} = \rho \frac{F_{S_0}}{\sigma_S} w_C \tag{86}$$

where $F_{S_0} = F_S(0)$.

The torque on the carrythrough structure is

$$T = M_0 \sin(\Lambda_S) \tag{87}$$

and the weight of the torsion material is then

$$W_{TORSION_C} = \frac{\rho T (t_0 + C_{SR}) w_C}{t_0 C_{SR} \sigma_S} \tag{88}$$

Finally, the *ideal* weight of the carrythrough structure is computed from a summation of the bending shear and torsion material, or

$$W_C = W_{BEND_C} + W_{SHEAR_C} + W_{TORSION_C} \tag{89}$$

As in the case of the fuselage structural weight, *nonoptimum* weight must be added to the ideal weight to obtain the true wing structural weight. The method used will be discussed below.

The static deflection of the wingtip under the pull-up maneuver is also determined. Using the moment-area method applied to an Euler beam (ref. 11), the deviation of point *B* on the deflected surface from the tangent drawn from another point *A* on the surface is equal to the area under the *M*/(*EI*) diagram between *A* and *B* multiplied by the distance to the centroid of this area from *B*,

$$t_{BA} = \int_B^A y d\theta = \int_B^A \frac{M}{EI} y dy \tag{90}$$

where θ is the angular displacement of the beam and *y* is the longitudinal axis of the beam. For the case of a wing with trapezoidal planform, the longitudinal axis, *y*, will lie along the quarter-chord line (fig. 3). For a wing with a horizontal unloaded configuration, the tangential deviation, t_{BA}, will equal the true vertical tip displacement (assumed to be the case). Only the wing cover contributes to the bending resistance, while the webs offer similar shear stiffness. The wing area moment of inertia, *I*, at any structural semispan station *y* is determined with the Parallel Axis theorem, as cover thickness is small when compared with total wing thickness.

Regression Analysis

Overview– Using fuselage and wing weight statements of eight subsonic transports, a relation between the calculated load-bearing structure weights obtained through PDCYL and the actual load-bearing structure weights, primary structure weights, and total weights is determined using statistical analysis techniques. A basic application which is first described is linear regression, wherein the estimated weights of the aircraft are related to the weights calculated by PDCYL with a straight line, $y = mx + b$, where *y* is the value of the estimated weight, *m* is the slope of the line, *x* is the value obtained through PDCYL, and *b* is the *y*-intercept. This line is termed a *regression* line, and is found by using the *method of least squares*, in which the sum of the squares of the residual errors between actual data points and the corresponding points on the regression line is minimized. Effectively, a straight line is drawn through a set of ordered pairs of data (in this case eight weights obtained through PDCYL and the corresponding actual weights) so that the aggregate deviation of the actual weights above or below this line is minimized. The estimated weight is therefore dependent upon the independent PDCYL weight.

As an example, if the form of the regression equation is linear, the estimated weight is

$$y_{est} = mx_{calc} + b \tag{91}$$

where *m* is the slope, *b* is the intercept, and x_{calc} is the weight PDCYL calculates. The resulting residual to be minimized is

$$E = \sum_{i=1}^{n} \left(y_{actual_i} - y_{est_i} \right)^2 \tag{92}$$

or

$$E = \sum_{i=1}^{n} \left(y_{actual_i} - mx_{calc_i} - b \right)^2 \tag{93}$$

where y_{actual} is the actual component weight and *n* is the number of aircraft whose data are to be used in the fit. By taking partial derivatives of the residual error with respect to both *m* and *b*, equations for the values of these two unknown variables are found to be

$$m = \frac{n \sum_{i=1}^{n} x_{calc_i} y_{act_i} - \sum_{i=1}^{n} x_{calc_i} \sum_{i=1}^{n} y_{act_i}}{n \sum_{i=1}^{n} x_{calc_i}^2 - \left(\sum_{i=1}^{n} x_{calc_i} \right)^2} \tag{94}$$

$$b = \bar{y}_{act} - n\bar{x}_{calc} \qquad \bar{x}, \bar{y} = \text{mean values of } x \text{ and } y \tag{95}$$

Of key importance is the degree of accuracy to which the prediction techniques are able to estimate actual aircraft weight. A measure of this accuracy, the correlation coefficient, denoted *R*, represents the reduction in residual error due to the regression technique. *R* is defined as

$$R = \sqrt{\frac{E_t - E_r}{E_r}} \tag{96}$$

where E_t and E_r refer to the residual errors associated with the regression before and after analysis is performed, respectively. A value of $R = 1$ denotes a perfect fit of the data with the regression line. Conversely, a value of $R = 0$ denotes no improvement in the data fit due to regression analysis.

There are two basic forms of equations which are implemented in this study. The first is of the form

$$y_{est} = mx_{calc} \tag{97}$$

The second general form is

$$y_{est} = mx_{calc}^{a} \tag{98}$$

The first form is a simplified version of the linear example as discussed above, with the *y*-intercept term set to zero. However, because the second general equation is not linear, nor can it be transformed to a linear equation, an alternative method must be employed. In order to formulate the resulting *power-intercept* regression equation, an iterative approach developed by D. W. Marquardt is utilized (ref. 12). This algorithm starts at a certain point in space, and, by applying the method of steepest descent, a gradient is obtained which indicates the direction in which the most rapid decrease in the residual errors will occur. In addition, the Taylor Series method produces a second similar vector. Interpolation between these two vectors yields a direction in which to move the point in order to minimize the associated error. After several iterations, the process converges to a minimum value. It should be noted that there may be several local minimums and there is no guarantee that the method converges to the global one.

Fuselage– The analysis above is used to develop a relationship between weight calculated by PDCYL and actual wing and fuselage weights. The data were obtained from detailed weight breakdowns of eight transport aircraft (refs. 13–17) and are shown in table 4 for the fuselage. Because the theory used in the PDCYL analysis only predicts the load-carrying structure of the aircraft components, a correlation between the predicted weight and the actual load-carrying structural weight and primary weight, as well as the total weight of the fuselage, was made.

Structural weight consists of all load-carrying members including bulkheads and frames, minor frames, covering, covering stiffeners, and longerons. For the linear curve-fit, the resulting regression equation is

$$W_{actual} = 1.3503 W_{calc} \qquad R = 0.9946 \qquad (99)$$

This shows that the *nonoptimum* factor for fuselage structure is 1.3503; in other words, the calculated weight must be increased by about 35 percent to get the actual structural weight. For the alternative power-intercept curve fitting analysis, the resulting load-carrying regression equation is

$$W_{actual} = 1.1304 W_{calc}^{1.0179} \qquad R = 0.9946 \qquad (100)$$

To use either of these equations to estimate total fuselage weight, nonstructural weight items must be estimated independently and added to the structural weight.

Primary weight consists of all load-carrying members as well as any secondary structural items such as joints fasteners, keel beam, fail-safe straps, flooring, flooring structural supplies, and pressure web. It also includes the lavatory structure, galley support, partitions, shear ties, tie rods, structural firewall, torque boxes, and attachment fittings. The linear curve fit for this weight yields the following primary regression equation

$$W_{actual} = 1.8872 W_{calc} \qquad R = 0.9917 \qquad (101)$$

The primary power-intercept regression equation is

$$W_{actual} = 1.6399 W_{calc}^{1.0141} \qquad R = 0.9917 \qquad (102)$$

Table 4. Fuselage weight breakdowns for eight transport aircraft

	Weight, lb			
Aircraft	PDCYL	Load-carrying structure	Primary structure	Total structure
B-720	6545	9013	13336	19383
B-727	5888	8790	12424	17586
B-737	3428	5089	7435	11831
B-747	28039	39936	55207	72659
DC-8	9527	13312	18584	24886
MD-11	20915	25970	34999	54936
MD-83	7443	9410	11880	16432
L-1011	21608	28352	41804	52329

The total fuselage weight accounts for all members of the body, including the structural weight and primary weight. It does not include passenger accommodations, such as seats, lavatories, kitchens, stowage, and lighting; the electrical system; flight and navigation systems; alighting gear; fuel and propulsion systems; hydraulic and pneumatic systems; the communication system; cargo accommodations; flight deck accommodations; air conditioning equipment; the auxiliary power system; and emergency systems. Linear regression results in the following total fuselage weight equation

$$W_{actual} = 2.5686 W_{calc} \qquad R = 0.9944 \qquad (103)$$

This shows that the nonoptimum factor for the total fuselage weight is 2.5686; in other words, the fuselage structure weight estimated by PDCYL must be increased by about 157 percent to get the actual total fuselage weight. This nonoptimum factor is used to compare fuselage structure weight estimates from PDCYL with total fuselage weight estimates from the Sanders and the Air Force equations used by ACSYNT.

The total fuselage weight power-intercept regression equation is

$$W_{actual} = 3.9089 W_{calc}^{0.9578} \qquad R = 0.9949 \qquad (104)$$

Plots of actual fuselage component weight versus PDCYL-calculated weight, as well as the corresponding linear regressions, are shown in figures 9–11.

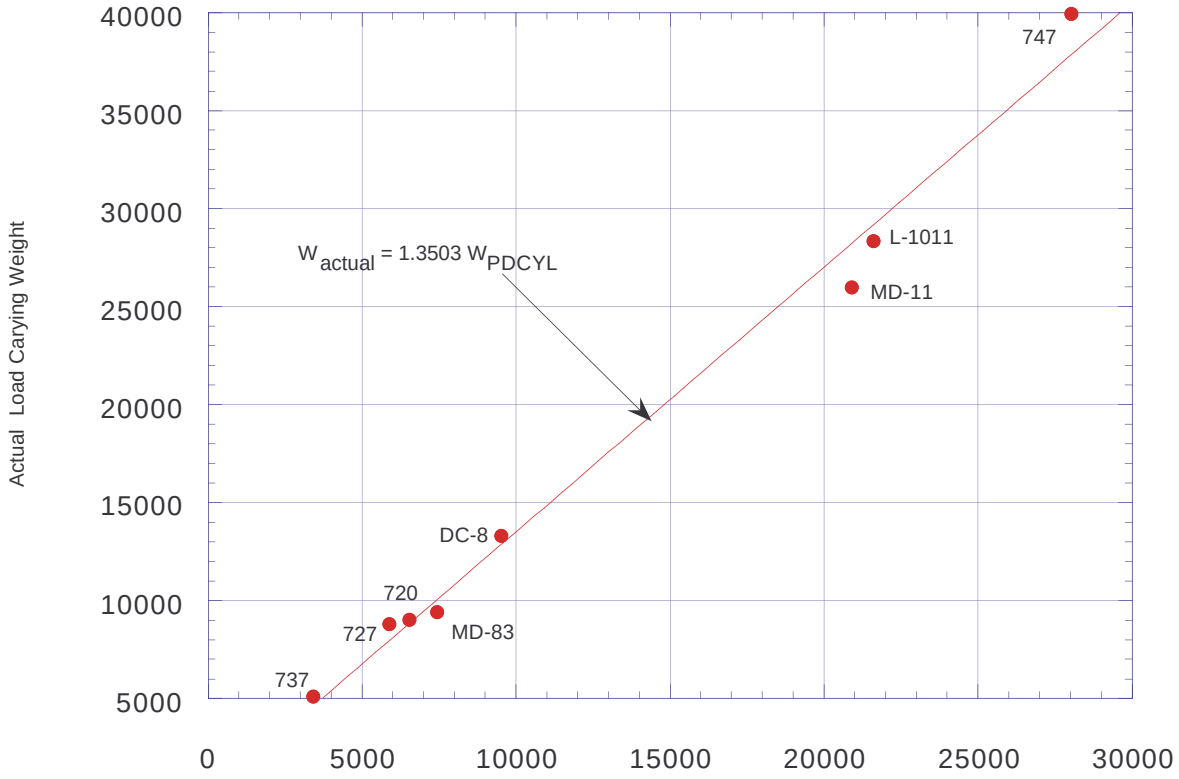

Figure 9. Fuselage load-carrying structure and linear regression.

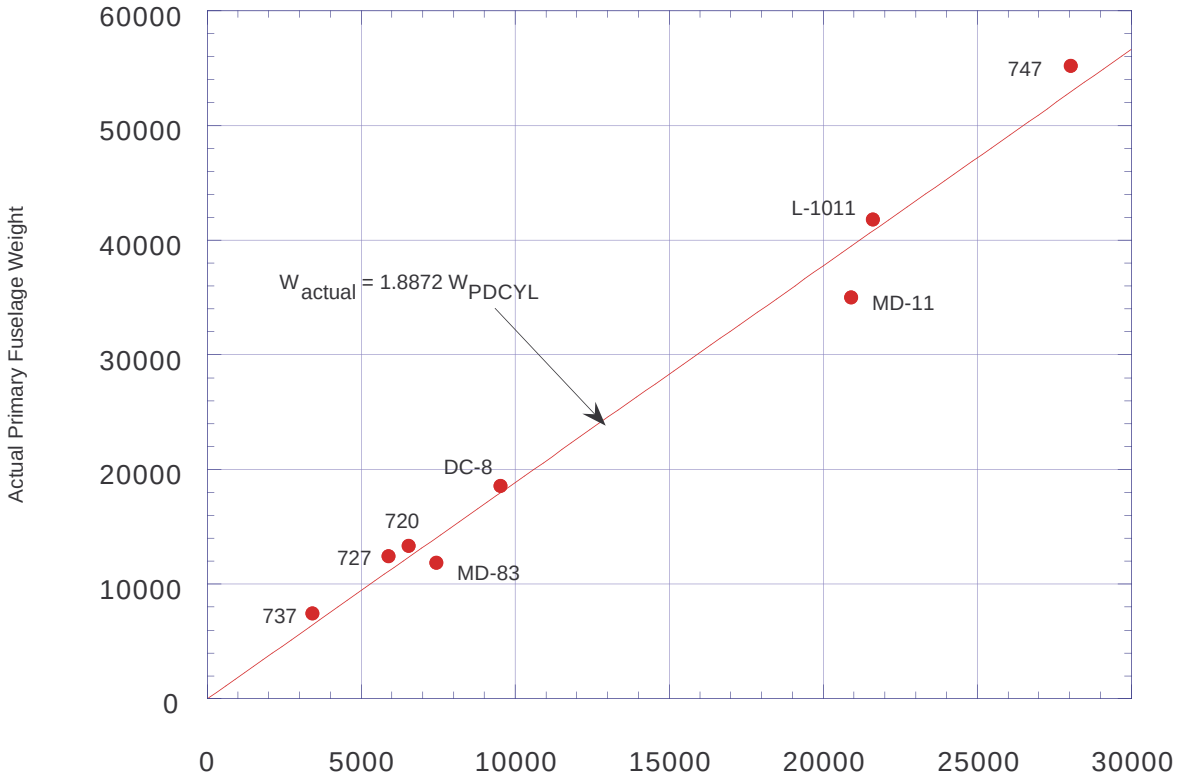

Figure 10. Fuselage primary structure and linear regression.

Figure 11. Fuselage total structure and linear regression.

Table 5. Wing weight breakdowns for eight transport aircraft

	Weight, lb			
Aircraft	PDCYL	Load-carrying structure	Primary structure	Total structure
B-720	13962	11747	18914	23528
B-727	8688	8791	12388	17860
B-737	5717	5414	7671	10687
B-747	52950	50395	68761	88202
DC-8	22080	19130	27924	35330
MD-11	33617	35157	47614	62985
MD-83	6953	8720	11553	15839
L-1011	25034	28355	36101	46233

Wing– The same analysis was performed on the wing weight for the sample aircraft and is shown in table 5. The wing box, or load-carrying structure, consists of spar caps, interspar coverings, spanwise stiffeners, spar webs, spar stiffeners, and interspar ribs. The wing box linear regression equation is

$$W_{actual} = 0.9843 W_{calc} \qquad R = 0.9898 \qquad (105)$$

so that the nonoptimum factor is 0.9843. Power-intercept regression results in

$$W_{actual} = 1.3342 W_{calc}^{0.9701} \qquad R = 0.9902 \qquad (106)$$

Wing primary structural weight includes all wing box items in addition to auxiliary spar caps and spar webs, joints and fasteners, landing gear support beam, leading and trailing edges, tips, structural firewall, bulkheads, jacket fittings, terminal fittings, and attachments. Linear regression results in

$$W_{actual} = 1.3442 W_{calc} \qquad R = 0.9958 \qquad (107)$$

Power-intercept regression yields

$$W_{actual} = 2.1926 W_{calc}^{0.9534} \qquad R = 0.9969 \qquad (108)$$

The total wing weight includes wing box and primary weight items in addition to high-lift devices, control surfaces, and access items. It does not include the propulsion system, fuel system, and thrust reversers; the electrical system; alighting gear; hydraulic and pneumatic systems; anti-icing devices; and emergency systems. The resulting total weight linear regression equation is

$$W_{actual} = 1.7372 W_{calc} \qquad R = 0.9925 \qquad (109)$$

This shows that the nonoptimum factor for the total wing weight is 1.7372; in other words, the wing box weight estimated by PDCYL must be increased by about 74 percent to get the actual total wing weight. This nonoptimum factor is used to compare wing box weight estimates from PDCYL with total wing weight estimates from the Sanders and the Air Force equations used by ACSYNT.

The power-intercept equation for total wing weight is

$$W_{actual} = 3.7464 W_{calc}^{0.9268} \qquad R = 0.9946 \qquad (110)$$

Plots of actual wing component weight versus PDCYL-calculated weight, as well as the corresponding linear regressions, are shown in figures 12–14.

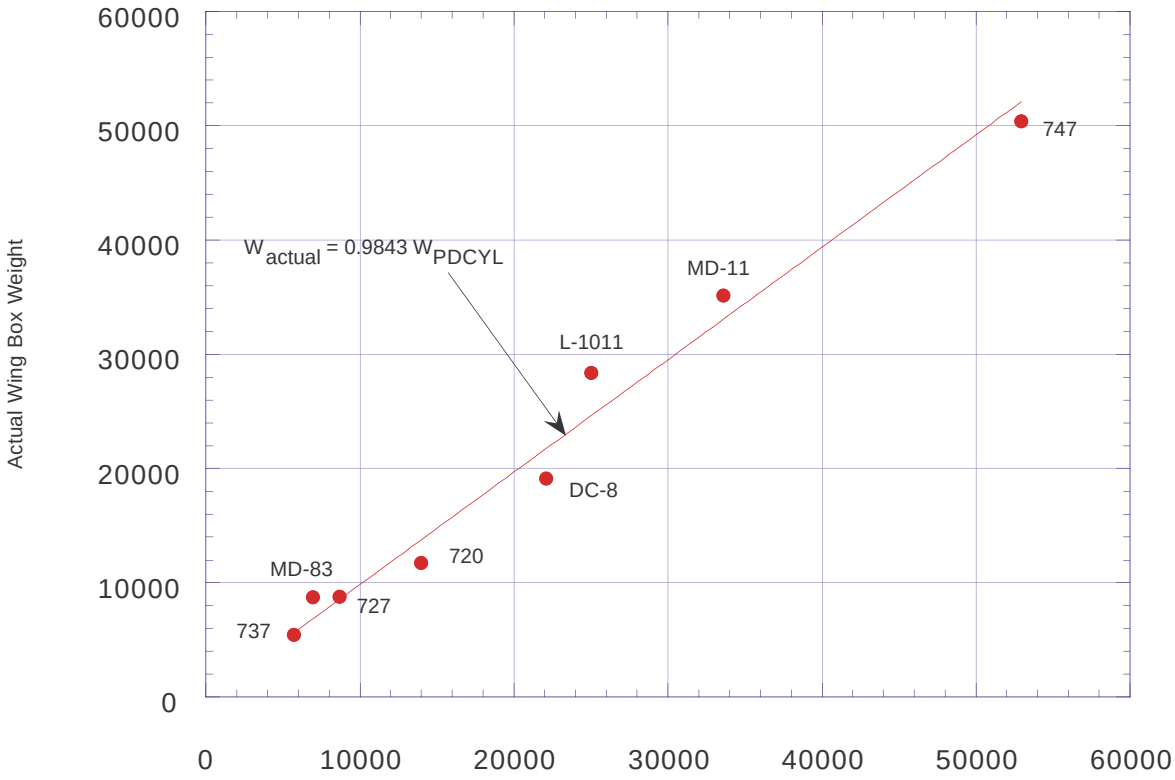

Figure 12. Wing load-carrying structure and linear regression.

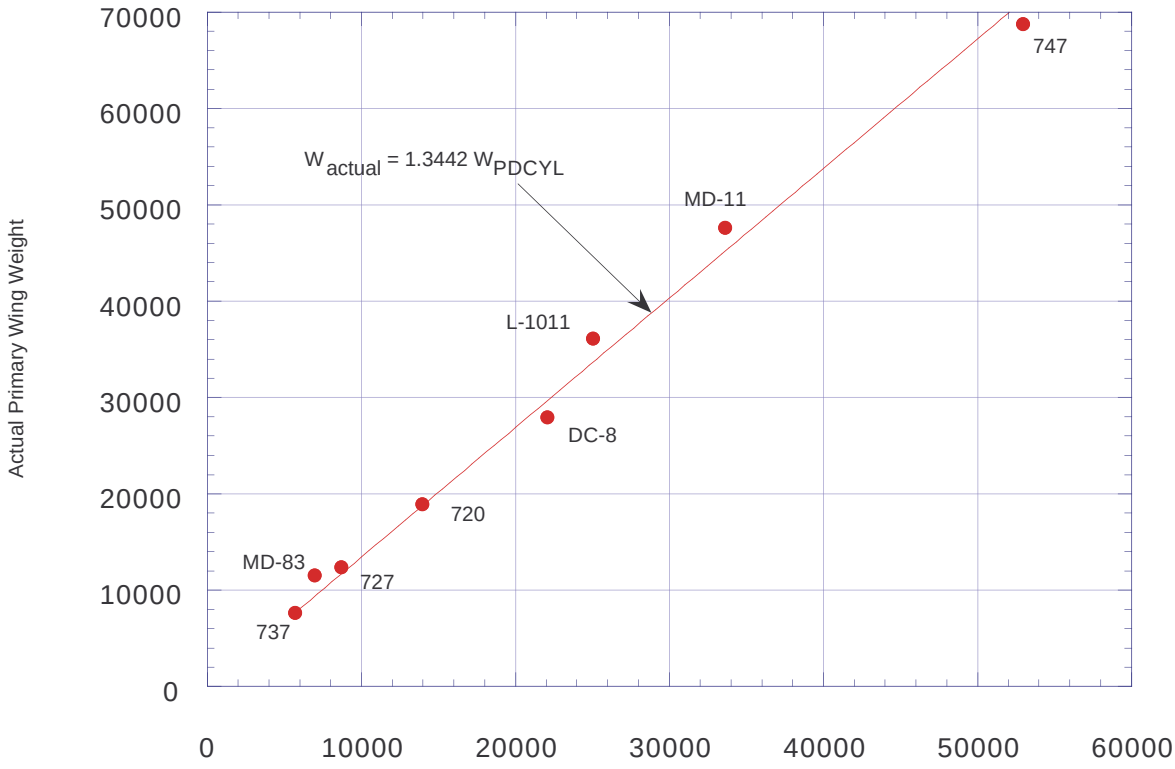

Figure 13. Wing primary structure and linear regression.

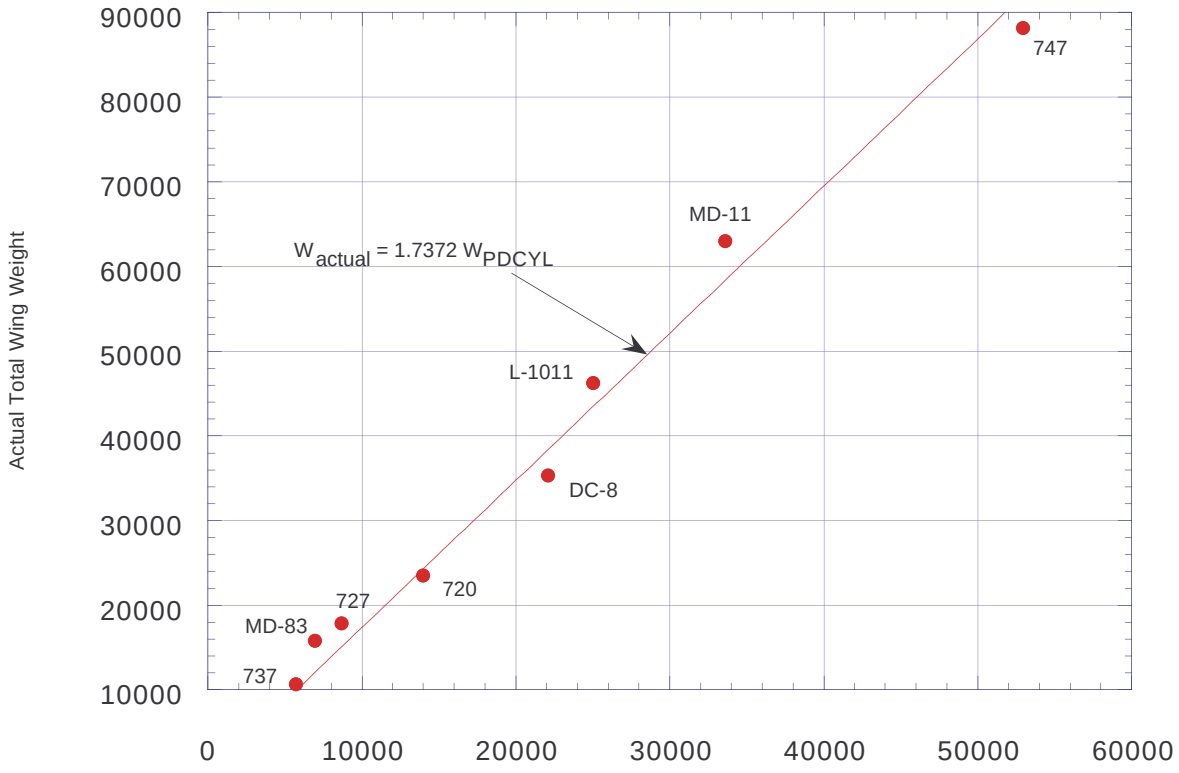

Figure 14. Wing total structure and linear regression.

Discussion– Both fuselage and wing weight linear and power regressions give excellent correlation with the respective weights of existing aircraft, as evidenced by the high values of the correlation coefficient, *R*. It should be noted that even though the power-based regressions give correlations equal to or better than the linear regressions their factors may vary distinctly from the linear cases. This is due to their powers not equaling unity.

Because estimates of non-load-bearing primary structure are generally not available at the conceptual design stage, and because nonprimary structure is probably not well estimated by a nonoptimum factor, equations 101 and 107 are recommended for estimating the primary structural weights of the respective transport fuselage and wing structures (figs. 10 and 13).

Appendix A – User's Manual, Example

Description

The purpose of this appendix is to give a detailed example of the input procedure used to allow PDCYL to calculate fuselage and wing weights for a sample transport aircraft during an ACSYNT run. A sample output from PDCYL will also be given. The Boeing 747-21P will be used for the example. The layout of the 747-21P is shown in figure 15. The weights of the load-carrying portions of the fuselage and wing box for the 747-21P will be calculated by PDCYL and scaled by the respective nonoptimum factors developed earlier to give estimates for the weights of the fuselage and wing. A comparison between methods currently used by ACSYNT to estimate fuselage and wing weights and PDCYL output will be made with the corresponding actual weights of the 747-21P.

Input

PDCYL requires input from both the existing ACSYNT data structure and an additional namelist containing data required by PDCYL which are not contained within the current ACSYNT format. There are three steps to run PDCYL within ACSYNT. First, the aircraft type is specified in the ACSYNT Control input. Currently the Transport Aircraft type is used. Second, data within ACSYNT module namelists are required. The ACSYNT Geometry, Trajectory, and Weights modules supply data for PDCYL execution. PDCYL uses the WING, HTAIL, VTAIL, FUS, WPOD, and FPOD namelists from the Geometry module. From the Trajectory module, the TRDATA namelist is used. From the Weights module the OPTS namelist is used. Third, data from the PDCYLIN namelist are used.

Variables used from ACSYNT namelists and the PDCYLIN namelist are given in tables 6 and 7, respectively. Default values for all variables are also given. These default values match the Boeing 747-21P. Key configuration parameters are given for each of the eight aircraft used in the validation study in table 8. An example of the PDCYLIN namelist input for the 747-21P is shown in figure 16.

A description of the specific structural concepts used to model both the fuselage and wing is given in the Structural Analysis section. As was noted earlier, the typical modern transport aircraft fuselage is a Z-stiffened shell. The buckling-minimum material gage compromise was employed because it gives the lowest-weight (optimal) structure for the eight aircraft investigated in this study.

Output

PDCYL weights output begins with the wing box and carrythrough structure analysis. The wing is sized during a quasi-static pull-up maneuver where the load factor is set equal to the ultimate load factor (nominally 3.75). Wing output contains three parts. First is the overall geometrical configuration. Second is a detailed station-by-station bending, shear, and torsion analysis and corresponding geometrical sizing along the span. Third is the detailed geometrical layout, loading, and weight breakdown of the carrythrough structure, weight breakdown of the wing components, and deflection of the wingtip. This wing weight is multiplied by the nonoptimum factor and returned to ACSYNT. An example of the PDCYL wing weight output for the 747-21P is shown in figure 17.

Next, the fuselage is analyzed. Fuselage output contains four parts. First is the overall geometrical layout and weight breakdown. Second is a station-by-station bending, shear, and axial stress analysis. Up to three load cases are investigated. In order they are a quasi-static pull-up maneuver, a landing maneuver, and travel over runway bumps. Third, the envelope of worst-case loading is shown for each station, from which the shell and frames are sized. Corresponding unit weight breakdowns are also given. As an option, the detailed geometric configuration at each station may be output. Fourth, weights summaries are given for the top and bottom sections of the fuselage (nominally the same). These summaries are then averaged to give the weight summary of the entire fuselage. The fuselage weight, including the corresponding nonoptimum factor, is returned to ACSYNT. An example of the PDCYL fuselage weight output for the 747-21P is shown in figure 18.

Figure 19(a) shows a comparison between fuselage weight estimates from the Sanders equation, the Air Force equation, and PDCYL with the actual fuselage weight of the 747-21P. Figure 19(b) shows a similar comparison for the wing weight. SLOPE and TECH factors were set to one for the comparisons in Figures 19(a) and 19(b), while the nonoptimum factors are those relating PDCYL estimations of structure weight to respective total component weight.

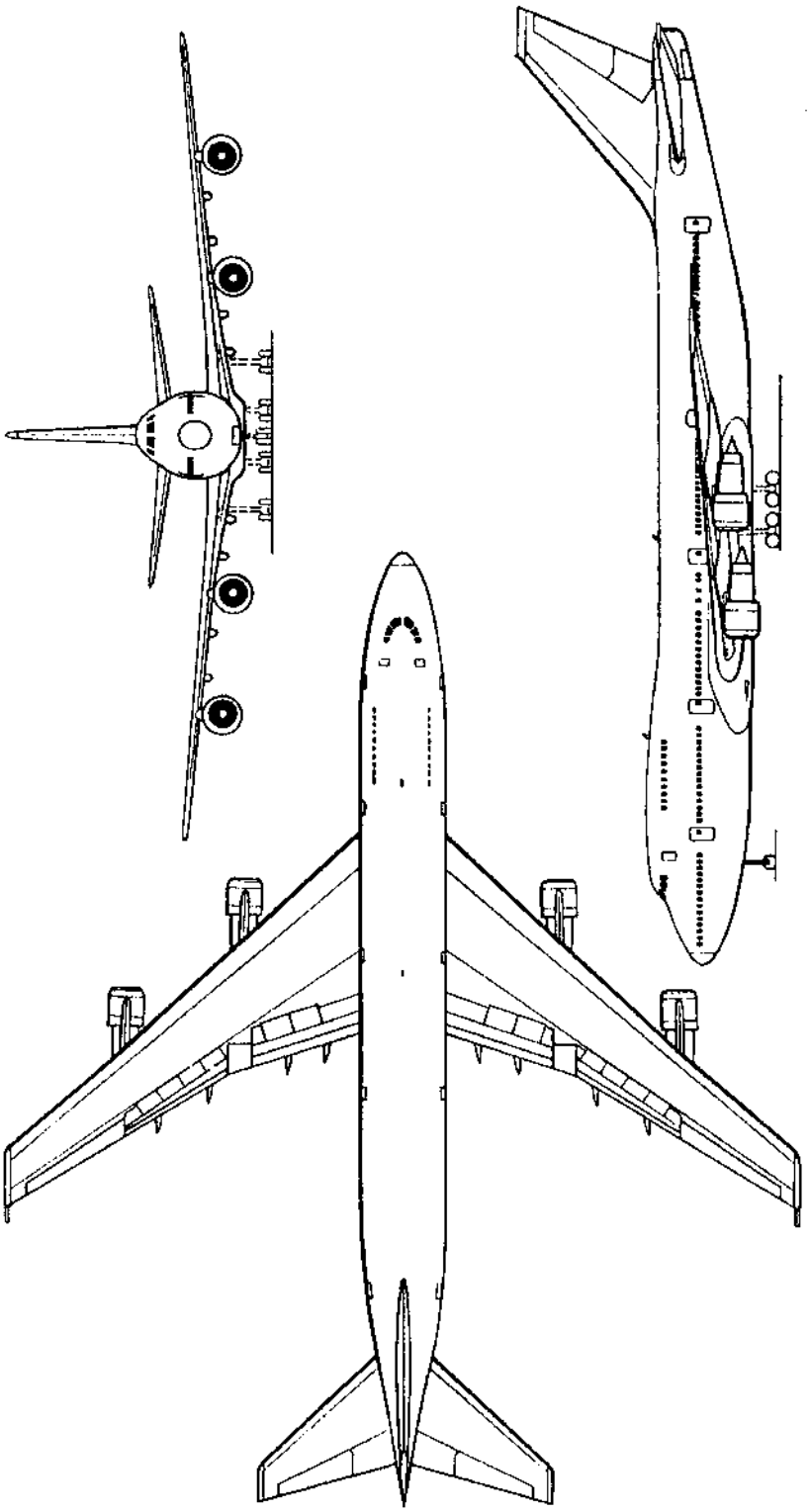

Figure 15. 747-21P configuration.

Table 6. ACSYNT variables

Variable	Type	Dimension	Description	Units/comment	Default (747)
1. Geometry module					
Namelist WING					
SWEEP	float	1	Sweep of wing.	degrees	37.17
KSWEEP	integer	1	1 → Referenced to the leading edge.		
			2 → Referenced to the quarter chord.		2
			3 → Referenced to the trailing edge.		
AR	float	1	Aspect ratio of wing.		6.96
TAPER	float	1	Taper ratio of wing.		0.2646
TCROOT	float	1	Thickness-to-chord ratio at the root.		0.1794
TCTIP	float	1	Thickness-to-chord ratio at the tip.		0.078
ZROOT	float	1	Elevation of MAC above fuselage reference plane, measured as a fraction of the local fuselage radius.		–0.1
AREA	float	1	Planform area of wing.	ft^2	5469
DIHED	float	1	Dihedral angle of wing.	degrees	7
XWING	float	1	Ratio of distance measured from nose to leading edge of wing to total fuselage length.		0.249
Namelist HTAIL (horizontal tail)					
SWEEP	float	1	Sweep of tail	degrees	34.29
KSWEEP	integer	1	1 → Referenced to the leading edge.		
			2 → Referenced to the quarter chord.		2
			3 → Referenced to the trailing edge.		
AR	float	1	Aspect ratio of the horizontal wing.	$(span)^2$/area	3.625
TAPER	float	1	Taper ratio of the horizontal wing.	tip chord/root chord	0.25
TCROOT	float	1	Thickness-to-chord ratio at the root.		0.11
TCTIP	float	1	Thickness-to-chord ratio at the tip.		0.08
ZROOT	float	1	Elevation of MAC above fuselage reference plane, measured as a fraction of the local fuselage radius.		0.69
AREA	float	1	Planform area of the horizontal wing.	ft^2	1470
XHTAIL	float	1	Position for trailing edge of tail root chord. If ZROOT ≤ 1, then XHTAIL is given as a fraction of body length. Else, XHTAIL is given as a fraction of the local vertical tail chord.		1

Table 6. Continued

Variable	Type	Dimension	Description	Units/comment	Default (747)
Namelist VTAIL (vertical tail)					
SWEEP	float	1	Sweep of vertical tail.	degrees	45.73
KSWEEP	integer	1	1 → Referenced to the leading edge.		
			2 → Referenced to the quarter chord.		2
			3 → Referenced t the trailing edge.		
AR	float	1	Aspect ratio of vertical tail.	$(\text{span})^2/\text{area}$	1.247
TAPER	float	1	Taper ratio of vertical tail.	tip chord/root chord	0.34
TCROOT	float	1	Thickness-to-chord ratio at root.		0.1298
TCTIP	float	1	Thickness-to-chord ratio at tip.		0.089
ZROOT	float	1	Elevation of MAC above fuselage reference plane, measured as a fraction of the local fuselage radius.		0.6
AREA	float	1	Planform area of vertical tail.	ft^2	830
Namelist FUS (fuselage)					
FRN	float	1	Fineness ratio of the nose section.	length/diameter	2.13
FRAB	float	1	Fineness ratio of after-body section.	length/diameter	3.29
BODL	float	1	Length of fuselage.	ft	225.167
BDMAX	float	1	Maximum diameter of fuselage.	ft	20.2
Namelist WPOD (wing-mounted propulsion pod)					
DIAM	float	1	Engine diameter.	ft	6.2
LENGTH	float	1	Length of engine pod.	ft	15
X	float	1	X location of nose of pod relative to leading edge of wing, given as a fraction of local chord of wing (>0 if face of pod is behind leading edge of wing).		–0.631
Y	float	1	Y location of center of pod, given as a fraction of semispan, measured from body centerline.		0.241
Z	float	1	Z location of center of pod above wing local chord, given as fraction of maximum pod diameter.		–0.83
SWFACT	float	1	Wetted area multiplier.		

Table 6. Concluded

Variable	Type	Dimension	Description	Units/comment	Default (747)
Namelist FPOD (fuselage-mounted propulsion pod)					
DIAM	float	1	Engine diameter.	ft	N/A
LENGTH	float	1	Length of engine pod.	ft	N/A
SOD	float	1	Stand-off-distance, the distance from the pod wall to the fuselage wall, given as a fraction of maximum pod radius.		N/A
THETA	float	1	Angular orientation of pod, THETA measured positive up from the horizontal reference plane.	degrees	N/A
X	float	1	X location of nose relative to nose of fuselage, given as a fraction of body length.		N/A
2. Trajectory module					
Namelist TRDATA (used for load factors)					
DESLF	float	1	Design load factor.	N/A	2.5
ULTLF	float	1	Ultimate load factor, usually 1.5*DESLF.	N/A	3.75
3. Weights module					
Namelist OPTS					
WGTO	float	1	Gross take-off weight.	lb	713000
WE	float	1	Total weight of propulsion system (includes both wing and fuselage mounted engines).	lb	44290

Table 7. PDCYL variables

Variable	Type	Dimension	Description	Units/comment	Default (747)
Namelist PDCYLIN					
Wing					
Material properties					
PS	float	1	Plasticity factor.		1
TMGW	float	1	Min. gage thickness for the wing	inches	0.2
EFFW	float	1	Buckling efficiency of the web.		0.656
EFFC	float	1	Buckling efficiency of the covers.		1.03
ESW	float	1	Young's Modulus for wing material.	psi	1.07E+07
FCSW	float	1	Ult. compressive strength of wing.	psi	54000
DSW	float	1	Density of the wing material.	$lb/in.^3$	0.101
KDEW	float	1	Knock-down factor for Young's Modulus.		1
KDFW	float	1	Knock-down factor for Ultimate strength.		1
Geometric parameters					
ISTAMA	integer	1	1 → the position of the wing is unknown. 2 → the position of the wing is known.		2
CS1	float	1	Position of structural wing box from leading edge as percent of root chord.		0.088
CS2	float	1	Position of structural wing box from trailing edge as percent of root chord.		0.277
Structural concept					
CLAQR	float	1	Ratio of body lift to wing lift.	For subsonic aircraft CLAQR ~ 0.0	0.001
IFUEL	integer	1	1 → no fuel is stored in the wing. 2 → fuel is stored in the wing.		2
CWMAN	float	1	Design maneuver load factor.		1
CF			Shanley's const. for frame bending.		6.25E-05
Fuselage					
Structural concept					
CKF	float	1	Frame stiffness coefficient.		5.24
EC	float	1	Power in approximation equation for buckling stability.		2.36
KGC	float	1	Buckling coefficient for component general buckling of stiffener web panel.		0.368
KGW	float	1	Buckling coefficient for component local buckling of web panel.		0.505

Table 7. Continued

KCON(T/B)	Structural geometry concept	Default (747)
2	Simply stiffened shell, frames, sized for minimum weight in buckling	
3	Z-stiffened shell, frames, best buckling	
4	Z-stiffened shell, frames, buckling-minimum gage compromise	
5	Z-stiffened shell, frames, buckling-pressure compromise	4
6	Truss-core sandwich, frames, best buckling	
8	Truss-core sandwich, no frames, best buckling	
9	Truss-core sandwich, no frames, buckling-min. gage-pressure compromise	

Variable	Type	Dimension	Description	Units/Comment	Default (747)
Material properties					
FTS(T/B)	float	4	Tensile strength on (top/bottom).	psi	58500
FCS(T/B)	float	4	Compressive strength.	psi	54000
ES(T/B)	float	4	Young's Modulus for the shells.	psi	1.07E+07
EF(T/B)	float	4	Young's Modulus for the frames.	psi	1.07E+07
DS(T/B)	float	4	Density of shell material on (t/b).	$lb/in.^3$	0.101
DF(T/B)	float	4	Density of frame material.	$lb/in.^3$	0.101
TMG(T/B)	float	4	Minimum gage thickness.	in.	0.071
KDE	float	1	Knock-down factor for modulus.		1
KDF	float	1	Knock-down factor for strength.		1
Geometric parameters					
CLBR1	float	1	Fuselage break point as a fraction of total fuselage length.		1.1
ICYL	integer	1	1 → modeled with a mid-body cylinder. Else → use two power-law bodies back to back.		1
Loads					
AXAC	float	1	Axial acceleration.	g's	0
CMAN	float	1	Weight fraction at maneuver.		1
ILOAD	integer	1	1 → analyze maneuver only. 2 → analyze maneuver and landing only. 3 → analyze bump, landing, and maneuver.		3
PG(T/B)	float	12	Fuselage gage pressure on (top/bot).	psi	13.65
WFBUMP	float	1	Weight fraction at bump.		0.001
WFLAND	float	1	Weight fraction at landing.		0.9

Table 7. Continued

Variable	Type	Dimension	Description	Units/Comment	Default (747)
Landing gear					
VSINK	float	1	Design sink velocity at landing.	ft/sec	10
STROKE	float	1	Stroke of landing gear.	ft	2.21
CLRG1	float	1	Length fraction of nose landing gear.		0.1131
CLRG2	float	1	Length fraction of main landing gear measured as a fraction of total fuselage length.		0.466
WFGR1	float	1	Weight fraction of nose landing gear.		0.0047
WFGR2	float	1	Weight fraction of main landing gear.		0.0398
IGEAR	integer	1	1 → main landing gear located on fuselage. 2 → main landing gear located on wing.		2
GFRL	float	1	Ratio of force taken by nose landing gear to force taken by main gear at landing.		0.001
CLRGW1 CLRGW2	float float	1 1	Position of wing gear as a fraction of structural semispan.	If only 1 wing gear, set CLRGW2 = 0.0	0.064 0.1844
Tails					
ITAIL	integer	1	1 → control surfaces mounted on tail. 2 → control surfaces mounted on wing.		1
Weights					
WTFF	float	1	Weight fraction of fuel.		0.262
CBUM	float	1	Weight fraction at bump.		1
CLAN	float	1	Weight fraction at landing.		0.791

Table 7. Concluded

Variable	Type	Dimension	Description	Units/Comment	Default (747)
Factors					
ISCHRENK	integer	1	1 → use Schrenk load distribution on wing. Else → use trapezoidal distribution.		1
ICOMND	integer	1	1 → print gross shell dimensions envelope. 2 → print detailed shell geometry.		1
WGNO	float	1	Nonoptimal factor for wing (including the secondary structure).		1
SLFMB	float	1	Static load factor for bumps.		1.2
WMIS	float	1	Volume component of secondary structure.		0
WSUR	float	1	Surface area component of secondary structure.		0
WCW	float	1	Factor in weight equation for nonoptimal weights.		1
WCA	float	1	Factor in weight equation multiplying surface areas for nonoptimal weights.		0
NWING	integer	1	Number of wing segments for analysis.		40

Table 8. Key configuration parameters for eight transport aircraft

Variable	720	727	737	747	DC-8	MD-11	MD-83	L-1011
ACSYNT INPUT PARAMETERS								
1. Geometry module								
Namelist WING								
SWEEP	35	32	25	37.17	30.6	35	24.16	35
KSWEEP	2	2	2	2	2	2	2	2
AR	6.958	7.67	8.21	6.96	7.52	7.5	9.62	6.98
TAPER	0.333	0.2646	0.2197	0.2646	0.1974	0.255	0.156	0.3
TCROOT	0.1551	0.154	0.126	0.1794	0.1256	0.167	0.138	0.13
TCTIP	0.0902	0.09	0.112	0.078	0.105	0.093	0.12	0.09
ZROOT	–1	–1	–0.25	–0.1	–1	–0.79	–1	–1
AREA	2460	1587	1005	5469	2927	3648	1270	3590
DIHED	3	3	6	7	3	6	3	3
XWING	0.2963	0.376	0.35	0.249	0.302	0.218	0.468	0.359
Namelist HTAIL								
SWEEP	35	31.05	30.298	34.29	35	35.5	30.8	3.5
KSWEEP	2	2	2	2	2	2	2	2
AR	3.15	3.4	4.04	3.625	4.04	3.43	4.88	4
TAPER	0.457	0.383	0.3974	0.25	0.329	0.412	0.357	0.33
TCROOT	0.11	0.11	0.132	0.11	0.095	0.143	0.107	0.095
TCTIP	0.09	0.0894	0.108	0.08	0.08	0.1067	0.08	0.08
ZROOT	0.5	2	0.67	0.69	0.25	0.6875	2	0.5
AREA	500	376	312	1470	559	920	314	1282
XHTAIL	1	0.95	0.8532	0.974	1	0.96	0.98	0.9265
Namelist VTAIL								
SWEEP	35	48.4	34.16	45.73	35	38	39.4	35
KSWEEP	2	2	2	2	2	2	2	2
AR	1.45	1.09	1.814	1.247	1.905	1.73	1.48	1.6
TAPER	0.484	0.641	0.3024	0.34	0.292	0.343	0.844	0.3
TCROOT	0.11	0.11	0.1322	0.1298	0.096	0.105	0.127	0.11
TCTIP	0.0896	0.09	0.1081	0.089	0.101	0.125	0.103	0.0896
ZROOT	0.95	0.2	0	0.6	0.95	0.85	0.9	0.95
AREA	312.4	356	225	830	352	605	550	550

Table 8. Continued

Variable	720	727	737	747	DC-8	MD-11	MD-83	L-1011
Namelist FUS								
FRN	1.81	2	1.915	2.13	2	1.67	1.15	1.76
FRAB	2.86	2.831	2.361	3.29	2.9375	2.27	2.73	2.96
BODL	130.5	116.67	90.58	225.167	153	192.42	135.5	177.67
BDMAX	14.21	14.2	13.167	20.2	13.5	19.75	11.44	19.583
Namelist WPOD (inboard)								
DIAM	3.24	N/A	3.542	6.2	4.42	9.04	N/A	3.24
LENGTH	12.15	N/A	10	15	12.15	18.08	N/A	12.15
X	0.917	N/A	–0.22	–0.631	–0.4	–0.558	N/A	–0.639
Y	0.386	N/A	0.343	0.241	0.352	0.33125	N/A	0.461
Z	–1	N/A	–0.548	–0.83	–1.2	–0.5	N/A	–1
SWFACT	1	N/A	1	1	1	1	N/A	1
Namelist WPOD (outboard)								
DIAM	3.24	N/A	N/A	6.2	4.42	N/A	N/A	N/A
LENGTH	12.15	N/A	N/A	15	12.15	N/A	N/A	N/A
X	0.917	N/A	N/A	–0.631	–0.955	N/A	N/A	N/A
Y	0.674	N/A	N/A	0.441	0.61	N/A	N/A	N/A
Z	–1	N/A	N/A	–0.83	–1.2	N/A	N/A	N/A
SWFACT	1	N/A	N/A	1	1	N/A	N/A	N/A
Namelist FPOD								
DIAM	N/A	3.542	N/A	N/A	N/A	9.04	6.6	3.24
LENGTH	N/A	10	N/A	N/A	N/A	40.68	20.34	12.15
SOD	N/A	0	N/A	N/A	N/A	0	0	0
THETA	N/A	90	N/A	N/A	N/A	90	0	90
X	N/A	0.699	N/A	N/A	N/A	0.812	0.746	0.725
SYMCOD	N/A	1	N/A	N/A	N/A	1	0	–1
Namelist FPOD (third engine)								
DIAM	N/A	3.542	N/A	N/A	N/A	N/A	N/A	N/A
LENGTH	N/A	10	N/A	N/A	N/A	N/A	N/A	N/A
SOD	N/A	0.2	N/A	N/A	N/A	N/A	N/A	N/A
THETA	N/A	14.8	N/A	N/A	N/A	N/A	N/A	N/A
X	N/A	0.699	N/A	N/A	N/A	N/A	N/A	N/A
SYMCOD	N/A	0	N/A	N/A	N/A	N/A	N/A	N/A

Table 8. Continued

Variable	720	727	737	747	DC-8	MD-11	MD-83	L-1011
2. Trajectory module								
Namelist TRDATA								
DESLF	2.5	2.5	2.5	2.5	2.5	2.5	2.5	2.5
ULTLF	3.75	3.75	3.75	3.75	3.75	3.75	3.75	3.75
3. Weights module								
Namelist OPTS								
WGTO	202000	160000	100800	713000	335000	602500	140000	409000
Namelist FIXW								
WE	18202	12759	8165	44290	27058	40955	10340	34797
PDCYL INPUT PARAMETERS								
Wing								
Geometric parameters								
ISTAMA	2	2	2	2	2	2	2	2
CS1	0.1	0.2125	0.0724	0.088	0.0818	0.168	0.181	0.093
CS2	0.27	0.25	0.238	0.277	0.136	0.2835	0.271	0.296
Structural concept								
CLAQR	0.001	0.001	0.001	0.001	0.001	0.001	0.001	0.001
IFUEL	2	2	2	2	2	2	2	2
CWMAN	1	1	1	1	1	1	1	1
CF	6.25E–05	6.25E–05	6.25E–05	6.25E–05	6.25E–05	6.25E–05	6.25E–05	6.25E–05
Material properties								
PS	1	1	1	1	1	1	1	1
TMGW	0.02	0.02	0.02	0.02	0.02	0.02	0.02	0.02
EFFW	0.656	0.656	0.656	0.656	0.656	0.656	0.656	0.656
EFFC	1.03	1.03	1.03	1.03	1.03	1.03	1.03	1.03
ESW	1.08E+07	1.08E+07	1.08E+07	1.07E+07	1.08E+07	1.07E+07	1.07E+07	1.06E+07
FCSW	63500	56000	56000	54000	56000	56000	56000	67000
DSW	0.101	0.101	0.101	0.101	0.101	0.101	0.101	0.101
KDEW	1	1	1	1	1	1	1	1
KDFW	1	1	1	1	1	1	1	1

Table 8. Continued

Variable	720	727	737	747	DC-8	MD-11	MD-83	L-1011
Fuselage								
Geometric parameters								
CLBR1	1.1	1.1	1.1	1.1	1.1	1.1	1.1	1.1
ICYL	1	1	1	1	1	1	1	1
Structural concept								
CKF	5.24	5.24	5.24	5.24	5.24	5.24	5.24	5.24
EC	2.36	2.36	2.36	2.36	2.36	2.36	2.36	2.36
KGC	0.368	0.368	0.368	0.368	0.368	0.368	0.368	0.368
KGW	0.505	0.505	0.505	0.505	0.505	0.505	0.505	0.505
Material properties								
FTS(T/B)	58500	58500	58500	58500	64000	58500	58500	58500
FCS(T/B)	54000	54000	54000	54000	39000	54000	54000	54000
ES(T/B)	1.07E+07	1.07E+07	1.07E+07	1.07E+07	1.07E+07	1.07E+07	1.07E+07	1.07E+07
EF(T/B)	1.07E+07	1.07E+07	1.07E+07	1.07E+07	1.07E+07	1.07E+07	1.07E+07	1.07E+07
DS(T/B)	0.101	0.101	0.101	0.101	0.101	0.101	0.101	0.101
DF(T/B)	0.101	0.101	0.101	0.101	0.101	0.101	0.101	0.101
TMG(T/B)	0.04	0.04	0.036	0.071	0.05	0.055	0.055	0.075
KDE	1	1	1	1	1	1	1	1
KDF	1	1	1	1	1	1	1	1
Loads								
AXAC	0	0	0	0	0	0	0	0
CMAN	1	1	1	1	1	1	1	1
ILOAD	3	3	3	3	3	3	3	3
PG(T/B)	12.9	12.9	11.25	13.65	13.155	11.5	12.5	12.6
WFBUMP	0.001	0.001	0.001	0.001	0.001	0.001	0.001	0.001
WFLAND	0.9	0.9	0.9	0.9	0.9	0.9	0.9	0.9

Table 8. Concluded

Variable	720	727	737	747	DC-8	MD-11	MD-83	L-1011
Landing gear								
VSINK	10	10	10	10	10	10	10	10
STROKE	1.67	1.167	1.167	2.21	1.375	1.9	1.67	2.17
CLRG1	0.133	0.1306	0.145	0.1131	0.108	0.141	0.055	0.161
CLRG2	0.51	0.5896	0.5254	0.466	0.499	0.57	0.597	0.56
WFGR1	0.00389	0.00725	0.0052	0.0047	0.0311	0.0031	0.004	0.005
WFGR2	0.036	0.0738	0.0382	0.0398	0.0742	0.0058	0.035	0.044
IGEAR	2	2	2	2	2	2	2	2
GFRL	0.001	0.001	0.001	0.001	0.001	0.001	0.001	0.001
CLRGW1	0.1675	0.1736	0.1846	0.064	0.14	0.2	0.148	0.232
CLRGW2	0	0	0	0.1844	0	0	0	0
Tails								
ITAIL	1	1	1	1	1	1	1	1
Weights								
WTFF	0.3263	0.2625	0.156	0.262	0.418	0.336	0.2795	0.246
CBUM	1	1	1	1	1	1	1	1
CLAN	0.813	0.859	0.972	0.791	0.7164	0.7137	0.9143	0.851
Factors								
ISCHRENK	1	1	1	1	1	1	1	1
ICOMND	1	1	1	1	1	1	1	1
WGNO	1	1	1	1	1	1	1	1
SLFMB	1.2	1.2	1.2	1.2	1.2	1.2	1.2	1.2
WMIS	0	0	0	0	0	0	0	0
WSUR	0	0	0	0	0	0	0	0
WCW	1	1	1	1	1	1	1	1
WCA	0	0	0	0	0	0	0	0
NWING	40	40	40	40	40	40	40	40

```
$PDCYLIN

      PS=1.,          TMGW=.02,       EFFW=.656,
      EFFC=1.03,      ESW=10.7E06,    FCSW=54000.,    DSW=0.101,
      KDEW=1.0,       KDFW=1.0,

      ISTAMA=2,       CS1=0.088,      CS2=0.277,

      CLAQR=.001,     IFUEL=2,        CWMAN=1.0,      CF=6.25E-05,
      CKF=5.24,       EC=2.36,        KGC=.368,       KGW=.505,

      FTST = 4*58500.,8*0.,           FTSB = 4*58500.,8*0.,
      FCST = 4*54000.,8*0.,           FCSB = 4*54000.,8*0.,
      EST = 4*10.70E06,8*0.,          ESB = 4*10.70E06,8*0.,
      EFT = 4*10.70E06,8*0.,          EFB = 4*10.70E06,8*0.,
      DST = 4*.101,8*0.,              DSB = 4*.101,8*0.,
      DFT = 4*.101,8*0.,              DFB = 4*.101,8*0.,
      TMGT = 4*.071,8*0.,             TMGB = 4*.071,8*0.,
      KDE = 0.9,                      KDF = 0.9,

      CLBR1=1.1,      ICYL = 1,

      KCONT = 12*4,   KCONB = 12*4,

      AXAC=0.,        CBUM=1.0,       CLAN=0.791,
      CMAN=1.0,       ILOAD=3,        PGB = 12*13.65,  PGT = 12*13.65,
      WFBUMP=0.001,   WFLAND=0.9,

      WTFF=0.262,

      VSINK=10.0,     STROKE=2.21,    CLRG1=.1131,    CLRG2=0.466,
      WFGR1=0.0047,   WFGR2=0.0398,   IGEAR=2,        GFRL=0.001,
      CLRGW1=0.064,   CLRGW2 =0.1844,

      ITAIL=1,

      ISCHRENK=1,     ICOMND=1,       WGNO=1.00,      SLFMB=1.2,
      WMIS=0.,        WSUR=0.,        WCW=1.0,        WCA=0.0,
      NWING=40,

$END
```

Figure 16. PDCYLIN namelist for 747-21P.

SPAN	BS	ROOTC	TIPC	TAPER	TRATWR	TRATW	TGAML	GAMT	GAMS	VWING	WFUEL	DENW
FT	FT	FT	FT				DEG.	DEG.	DEG.	FT3	LBS	LB/FT3
195.1006	114.493	41.4650	11.0904	0.247	0.179	0.078	42.98067	30.30835	40.200	28673.285	186806.00	8.226

WING STATION FT	CHORD FT	LENGTH PRIME FT	LENGTH FT	BEND MOM FT-LBS	WEB SPACE IN	COVER THICK IN	WEB THICK IN	CGAGE THICK IN	WGAGE THICK IN	UNITWT COVERS LB/FT2	UNITWT WEBS LB/FT2	NJW
114.493	11.0904	5.4566	5.4566	4288.	0.4491	0.0543	0.03960	0.0200	0.02000	0.7904	0.5760	3
111.631	11.8497	5.8733	5.8733	27083.	0.7541	0.0543	0.03960	0.0200	0.02000	0.7904	0.5760	3
108.769	12.6091	6.2901	6.2901	77924.	1.0254	0.0543	0.03960	0.0200	0.02000	0.7904	0.5760	3
105.906	13.3684	6.7069	6.7069	162376.	1.2780	0.0543	0.03960	0.0200	0.02000	0.7904	0.5760	3
103.044	14.1278	7.1236	7.1236	284756.	1.5198	0.0543	0.03960	0.0200	0.02000	0.7904	0.5760	3
100.182	14.8872	7.5404	7.5404	448647.	1.7549	0.0680	0.03960	0.0250	0.02000	0.9893	0.5760	5
97.319	15.6465	7.9572	7.9572	657153.	1.9857	0.0874	0.03960	0.0322	0.02000	1.2710	0.5760	5
94.457	16.4059	8.3739	8.3739	912984.	2.2139	0.1071	0.03960	0.0394	0.02000	1.5579	0.5760	5
91.595	17.1653	8.7907	8.7907	1218559.	2.4403	0.1268	0.03960	0.0467	0.02000	1.8442	0.5760	5
88.732	17.9246	9.2075	9.2075	1576052.	2.6658	0.1462	0.03960	0.0538	0.02000	2.1260	0.5760	5
85.870	18.6840	9.6242	9.6242	1987387.	2.8907	0.1650	0.03960	0.0607	0.02000	2.4002	0.5760	5
83.008	19.4434	10.0410	10.0410	2454326.	3.1155	0.1832	0.03960	0.0674	0.02000	2.6648	0.5760	5
80.145	20.2027	10.4578	10.4578	2978392.	3.3404	0.2007	0.03960	0.0738	0.02000	2.9183	0.5760	5
77.283	20.9621	10.8745	10.8745	3561009.	3.5655	0.2173	0.03960	0.0800	0.02000	3.1600	0.5760	5
74.421	21.7215	11.2913	11.2913	4203376.	3.7911	0.2330	0.03960	0.0858	0.02000	3.3893	0.5760	5
71.558	22.4808	11.7081	11.7081	4906548.	4.0172	0.2479	0.03960	0.0912	0.02000	3.6061	0.5760	5
68.696	23.2402	12.1248	12.1248	5671446.	4.2439	0.2620	0.03960	0.0964	0.02000	3.8102	0.576	5
65.834	23.9996	12.5416	12.5416	6498817.	4.4712	0.2752	0.03960	0.1013	0.02000	4.0019	0.5760	5
62.971	24.7589	12.9584	12.9584	7389297.	4.6992	0.2875	0.03960	0.1058	0.02000	4.1812	0.5760	5
60.109	25.5183	13.3751	13.3751	8343357.	4.9278	0.2990	0.03960	0.1100	0.02000	4.3487	0.5760	5
57.247	26.2777	13.7919	13.7919	9361318.	5.1571	0.3097	0.03960	0.1140	0.02000	4.5046	0.5760	5
54.384	27.0370	14.2087	14.2087	10443365.	5.3870	0.3197	0.03960	0.1176	0.02000	4.6493	0.5760	5
51.522	27.7964	14.6254	14.6254	11589554.	5.6176	0.3289	0.03960	0.1210	0.02000	4.7832	0.5760	5
48.660	28.5557	15.0422	15.0422	12799800.	5.8487	0.3374	0.03960	0.1242	0.02000	4.9068	0.5760	5
45.797	29.3151	15.4590	15.4590	14073814.	6.0805	0.3452	0.03960	0.1270	0.02000	5.0204	0.5760	5
42.935	30.0745	15.8757	15.8757	15404417.	6.3119	0.3522	0.03960	0.1296	0.02000	5.1221	0.5760	5
40.073	30.8338	16.2925	16.2925	16685894.	6.5323	0.3562	0.03960	0.1311	0.02000	5.1803	0.5760	5
37.210	31.5932	16.7093	16.7093	18029610.	6.7542	0.3599	0.03960	0.1324	0.02000	5.2344	0.5760	5
34.348	32.3526	17.1260	17.1260	19434718.	6.9775	0.3633	0.03960	0.1337	0.02000	5.2844	0.5760	5
31.486	33.1119	17.5428	17.5428	20900252.	7.2020	0.3665	0.03960	0.1349	0.02000	5.3299	0.5760	5
28.623	33.8713	17.9596	17.9596	22425084.	7.4274	0.3693	0.03960	0.1359	0.02000	5.3710	0.5760	5
25.761	34.6307	18.3763	18.3763	24007966.	7.6538	0.3718	0.03960	0.1368	0.02000	5.4075	0.5760	5
22.899	35.3900	18.7931	18.7931	25647446.	7.8809	0.3740	0.03960	0.1376	0.02000	5.4394	0.5760	5
20.036	36.1494	19.2099	19.1785	27341956.	8.1086	0.3759	0.03960	0.1383	0.02000	5.4667	0.5760	5
17.174	36.9088	19.6266	17.1275	29070202.	8.3352	0.3772	0.03960	0.1388	0.02000	5.4857	0.5760	5
14.312	37.6681	20.0434	15.0765	30734100.	8.5538	0.3768	0.03960	0.1387	0.02000	5.4800	0.5760	5
11.449	38.4275	20.4602	13.0255	32427216.	8.7716	0.3760	0.03960	0.1384	0.02000	5.4691	0.5760	5
8.587	39.1869	20.8769	10.9744	34141228.	8.9884	0.3749	0.03960	0.1380	0.02000	5.4522	0.5760	5
5.725	39.9462	21.2937	8.9234	35868788.	9.2037	0.3733	0.03960	0.1374	0.02000	5.4291	0.5760	5
2.862	40.7056	21.7105	6.8724	37603512.	9.4172	0.3713	0.03960	0.1366	0.02000	5.3997	0.5760	5
0.000	41.4650	22.1272	4.8214	39330520.	9.6282	0.3687	0.03960	0.1357	0.02000	5.3630	0.5760	5

CLBOX1	CLINT	CLINTP	LBOX	WBOX	TBOX	NJW	WEBSB	TORK	TTO	TBCOV	SPLAN
FT	FT	FT	FT	FT	FT		FT	FT-LBS	IN	IN	FT2.
56.067	65.170	91.500	26.3302	20.2000	7.439	5	0.7127	18967352.0	0.0747	0.124	55469.

WSHEAR LBS	WBEND LBS	WWING LBS	WSHBOX LBS	WBDBOX LBS	WTOBOX LBS	WWBOX LBS	WWINGT LBS	WPOD LBS	DELTIP FT	CONTROL AREA FT2.	STRUCTURE AREA FT2.
885.00	18880.09	39530.17	280.72	7991.59	1482.61	9754.92	49285.09	11072.50	8.312	1535.09	3450.32

Figure 17. PDCYL wing weight output for 747-21P

FUSE STAT FT	BENDING MOMENT FT LBS	THIC STRESS IN	SHELL THICK PSI	EQUIV THICK IN	GAGE SPACE IN	FRAME AREA IN	NJ UNITWT	SECTION SQ FT	SHELL UNITWT LB/FT2	FRAME BENDING LB/FT2	MAX TYPE
3.7528	4516.695	0.0000	44.5238	0.1448	0.0710	23797.0703	3	58.3945	2.1055	0.0000	MAN
7.5056	29328.754	0.0000	178.2442	0.1448	0.0710	5944.2905	3	94.7155	2.1055	0.0000	MAN
11.2584	87603.664	0.0000	401.2114	0.1448	0.0710	2640.8411	3	125.6875	2.1055	0.0000	MAN
15.0111	190409.281	0.0000	713.4453	0.1448	0.0710	1485.0968	3	153.6281	2.1055	0.0001	MAN
18.7639	347701.844	0.0000	1114.9587	0.1448	0.0710	950.2913	3	179.5111	2.1055	0.0002	MAN
22.5167	568694.500	0.0000	1605.7603	0.1448	0.0710	659.8342	3	203.8644	2.1055	0.0005	MAN
26.2695	872144.000	0.0000	2211.4465	0.1448	0.0710	479.1142	3	227.0152	2.1055	0.0010	MAN
30.0223	1293259.875	0.0000	2987.5078	0.1448	0.0710	354.6553	3	249.1838	2.1055	0.0020	MAN
33.7751	1802858.500	0.0000	3836.1211	0.1448	0.0710	276.1997	3	270.5282	2.1055	0.0037	MAN
37.5278	2408529.000	0.0000	4761.6157	0.1448	0.0710	222.5160	3	291.1660	2.1055	0.0061	MAN
41.2806	3117610.000	0.0000	5766.8906	0.1448	0.0710	183.7273	3	311.1883	2.1055	0.0095	MAN
45.0334	3937044.500	0.0000	7075.2378	0.1448	0.0710	149.7526	3	320.3114	2.1055	0.0147	MAN
48.7862	4870150.000	0.0000	8752.1152	0.1448	0.0710	121.0605	3	320.3114	2.1055	0.0225	MAN
52.5390	5917042.000	0.0000	10633.4785	0.1448	0.0710	99.6415	3	320.3114	2.1055	0.0332	MAN
56.2918	7077723.000	0.0000	12719.3301	0.1448	0.0710	83.3012	3	320.3114	2.1055	0.0476	MAN
60.0445	8352191.000	0.0000	15009.6689	0.1448	0.0710	70.5902	3	320.3114	2.1055	0.0662	MAN
63.7973	9740450.000	0.0000	17504.5000	0.1448	0.0710	60.5293	3	320.3114	2.1055	0.0901	MAN
67.5501	11718714.000	0.0000	21059.6289	0.1448	0.0710	50.3112	3	320.3114	2.1055	0.1304	MAN
71.3029	15602571.000	0.0000	28039.2813	0.1448	0.0710	37.7875	3	320.3114	2.1055	0.2311	MAN
75.0557	20633438.000	0.0000	37080.2188	0.1448	0.0710	28.5741	3	320.3114	2.1055	0.4042	MAN
78.8085	25873488.000	0.0000	46497.0820	0.1448	0.0710	22.7871	3	320.3114	2.1055	0.6356	MAN
82.5612	30384872.000	0.0000	47662.5430	0.1659	0.0813	25.4677	6	320.3114	2.4122	0.5829	MAN
86.3140	33229772.000	0.0000	48052.2500	0.1799	0.0882	27.4022	6	320.3114	2.6166	0.5462	MAN
90.0668	33470324.000	0.0000	48082.4258	0.1811	0.0888	27.5660	6	320.3114	2.6339	0.5433	MAN
93.8196	30972306.000	0.0000	47748.3359	0.1688	0.0828	25.8668	6	320.3114	2.4544	0.5750	MAN
97.5724	28304028.000	0.0000	47332.9063	0.1556	0.0763	24.0551	6	320.3114	2.2626	0.6129	MAN
101.3252	25749524.000	0.0000	46274.3086	0.1448	0.0710	22.8968	3	320.3114	2.1055	0.6295	MAN
105.0780	23308814.000	0.0000	41888.1211	0.1448	0.0710	25.2944	3	320.3114	2.1055	0.5158	MAN
108.8307	20981884.000	0.0000	37706.4102	0.1448	0.0710	28.0996	3	320.3114	2.1055	0.4180	MAN
112.5835	18768758.000	0.0000	33729.2148	0.1448	0.0710	31.4130	3	320.3114	2.1055	0.3344	MAN
116.3363	16843416.000	0.0000	30269.1953	0.1448	0.0710	35.0038	3	320.3114	2.1055	0.2693	LAN
120.0891	15216945.000	0.0000	27346.2754	0.1448	0.0710	38.7451	3	320.3114	2.1055	0.2198	LAN
123.8419	13674075.000	0.0000	24573.5938	0.1448	0.0710	43.1168	3	320.3114	2.1055	0.1775	LAN
127.5947	12214827.000	0.0000	21951.1875	0.1448	0.0710	48.2678	3	320.3114	2.1055	0.1417	LAN
131.3474	10839192.000	0.0000	19479.0430	0.1448	0.0710	54.3936	3	320.3114	2.1055	0.1115	LAN
135.1002	9547162.000	0.0000	17157.1445	0.1448	0.0710	61.7548	3	320.3114	2.1055	0.0865	LAN
138.8530	8338768.500	0.0000	14985.5488	0.1448	0.0710	70.7038	3	320.3114	2.1055	0.0660	LAN
142.6058	7213962.000	0.0000	12964.1660	0.1448	0.0710	81.7280	3	320.3114	2.1055	0.0494	LAN
146.3586	6172785.000	0.0000	11093.0723	0.1448	0.0710	95.5133	3	320.3114	2.1055	0.0362	LAN

Figure 18. PDCYL fuselage weight output for 747-21P.

150.1113	5215206.000	0.0000	9372.2129	0.1448	0.0710	113.0507	3	320.3114	2.1055	0.0258	LAN
153.8641	4341246.000	0.0000	7801.6255	0.1448	0.0710	135.8096	3	320.3114	2.1055	0.0179	LAN
157.6169	3550887.000	0.0000	6381.2769	0.1448	0.0710	166.0382	3	320.3114	2.1055	0.0120	LAN
161.3697	2837451.000	0.0000	5246.6328	0.1448	0.0710	201.9458	3	311.3084	2.1055	0.0079	LAN
165.1224	2213004.000	0.0000	4268.8013	0.1448	0.0710	248.2045	3	298.4142	2.1055	0.0050	LAN
168.8752	1666440.000	0.0000	3362.5671	0.1448	0.0710	315.0972	3	285.2738	2.1055	0.0030	LAN
172.6280	1307928.000	0.0000	2769.3157	0.1448	0.0710	382.5983	3	271.8658	2.1055	0.0019	BUM
176.3808	1530244.500	0.0000	3411.9824	0.1448	0.0710	310.5337	3	258.1649	2.1055	0.0028	MAN
180.1335	1753683.000	0.0000	4134.7847	0.1448	0.0710	256.2493	3	244.1414	2.1055	0.0038	MAN
183.8863	1890422.250	0.0000	4736.1792	0.1448	0.0710	223.7110	3	229.7597	2.1055	0.0047	MAN
187.6391	1945607.250	0.0000	5209.6304	0.1448	0.0710	203.3802	3	214.9767	2.1055	0.0054	MAN
191.3919	1924485.000	0.0000	5546.1831	0.1448	0.0710	191.0387	3	199.7393	2.1055	0.0056	MAN
195.1447	1832528.250	0.0000	5733.5396	0.1448	0.0710	184.7960	3	183.9802	2.1055	0.0056	MAN
198.8974	1675338.750	0.0000	5753.5972	0.1448	0.0710	184.1518	3	167.6125	2.1055	0.0051	MAN
202.6502	1458795.000	0.0000	5578.8437	0.1448	0.0710	189.9203	3	150.5197	2.1055	0.0043	MAN
206.4030	1188949.500	0.0000	5163.7246	0.1448	0.0710	205.1882	3	132.5389	2.1055	0.0032	MAN
210.1558	872269.500	0.0000	4426.6021	0.1448	0.0710	239.3564	3	113.4288	2.1055	0.0020	MAN
213.9085	515652.000	0.0000	3198.5554	0.1448	0.0710	331.2544	3	92.7996	2.1055	0.0009	MAN
217.6613	126475.500	0.0000	1041.0522	0.1448	0.0710	1017.7543	3	69.9322	2.1055	0.0001	MAN
221.4141	46821.000	0.0000	625.1013	0.1448	0.0710	1694.9822	3	43.1155	2.1055	0.0000	MAN
221.4141	45793.500	0.0000	611.3832	0.1448	0.0710	1694.9822	3	43.1155	2.1055	0.0000	NONE

STRUCTURAL WEIGHT SUMMARY

	WEIGHT (LBS) (LBS/FT*FT)	WEIGHT FRACTION	UNIT WEIGHT
SHELL	26671.41	0.0374	2.1409
FRAMES	1837.49	918.7455	0.1475
NONOP	0.00	0.0000	0.0000
SEC	0.00	0.0000	0.0000
TOTAL	28508.89	0.0400	2.2884
VOLPEN	0.00	0.0000	0.0000
GRANTOT	28508.89	0.0400	2.2884

Surface Area, SQF	12457.98
Volume Ratio	1.00000000
BODY WEIGHT	28508.89453125

Figure 18. Concluded.

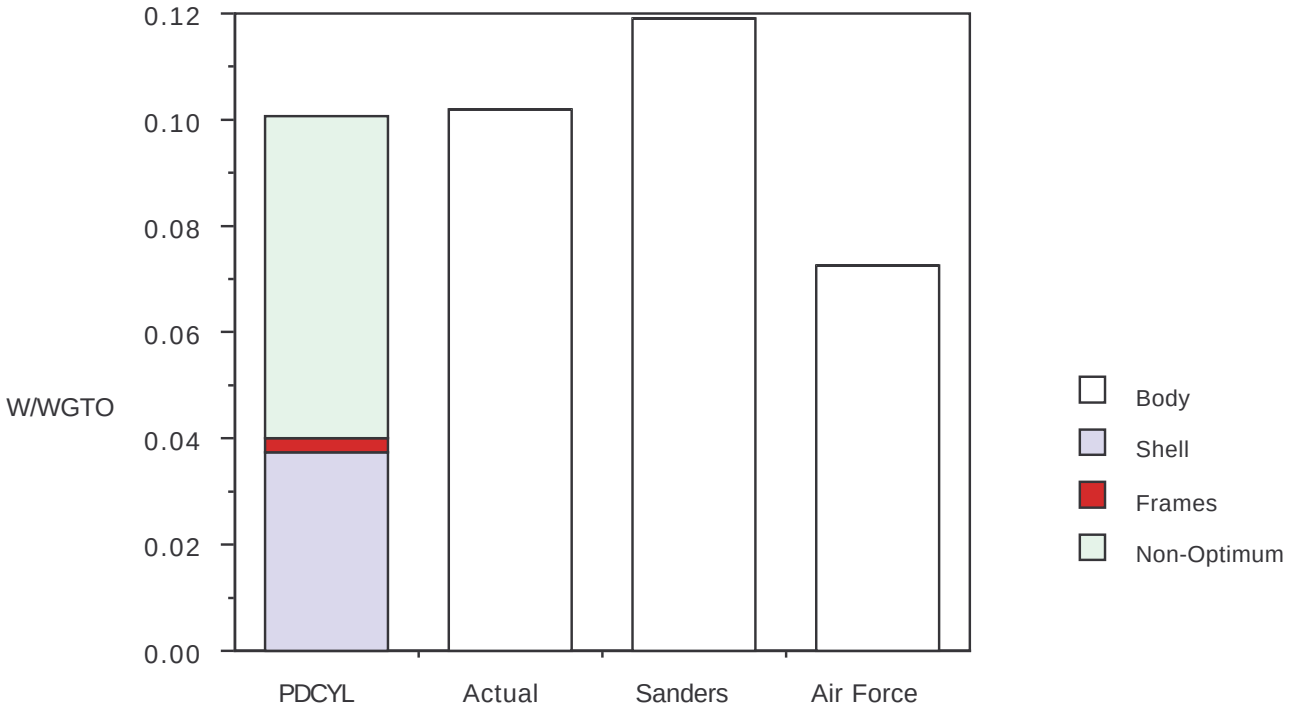

Figure 19(a). Fuselage weight estimation comparison for 747-21P.

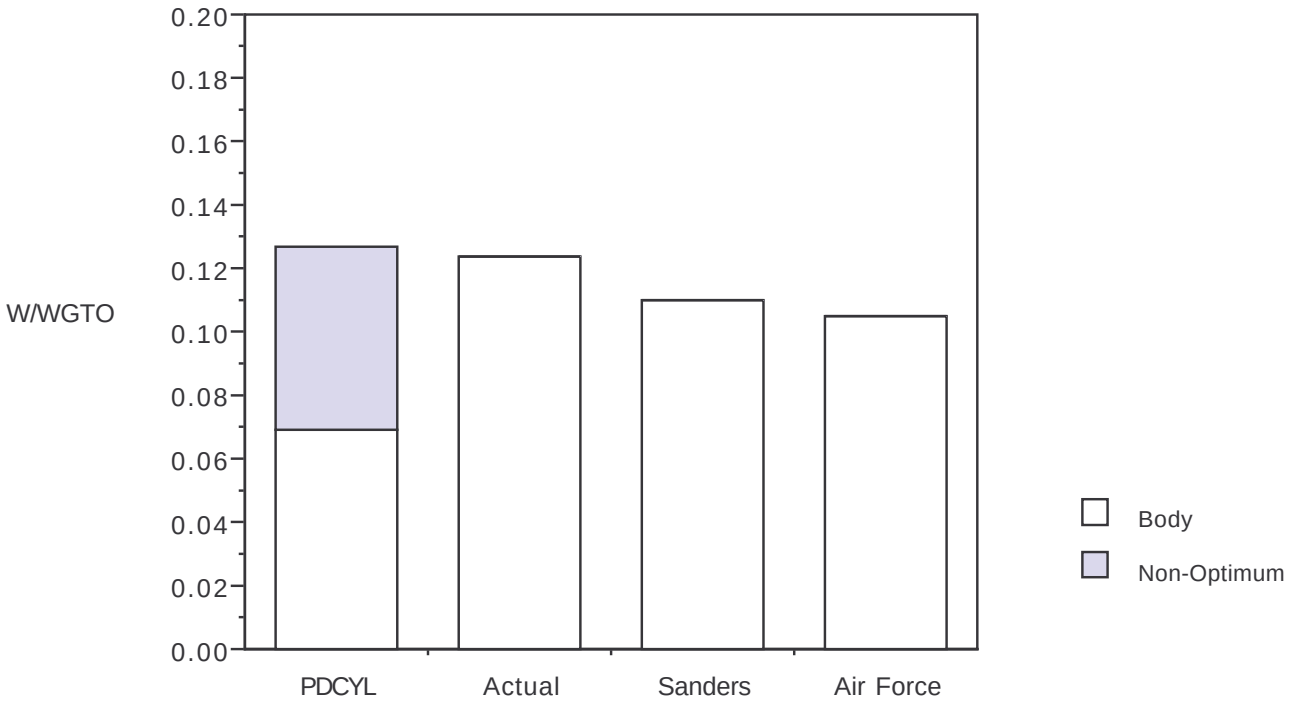

Figure 19(b). Wing weight estimation comparison for 747-21P.

Appendix B – High-Altitude Study

Description

A study was made to estimate the wing weight of a scaled version of an existing propeller-driven high-altitude drone aircraft. This aircraft, termed the Strato7, is modeled as an enlarged version of the existing Perseus-a3. PDCYL was used to validate the wing weight estimation returned by ACSYNT.

The wing of the Strato7 incorporates a single hollow, cylindrical carbon-fiber/epoxy spar placed at the leading edge. The strength of the cover is assumed negligible. No fuel is carried in the wing, while propulsion and landing gear are mounted on the fuselage. The layout of the Strato7 is shown in figure 20.

Input

Fuselage weight estimation is not considered for the Strato7. An example of the ACSYNT input for the Strato7 wing weight estimation is shown in figure 21. The corresponding PDCYLIN namelist for the case where the ratio of structural chord to total chord is 0.2 is shown in figure 22.

Output

Wing weight as a function of the ratio of structural chord to total chord is shown in figure 23. The wing weight estimated by ACSYNT is 789 pounds. PDCYL matches this wing weight when the ratio of structural chord to total chord is approximately 0.25. Nonoptimum weight was not considered in this analysis. In order to estimate nonoptimum weight, nonoptimum factors would need to be recomputed for this type of aircraft.

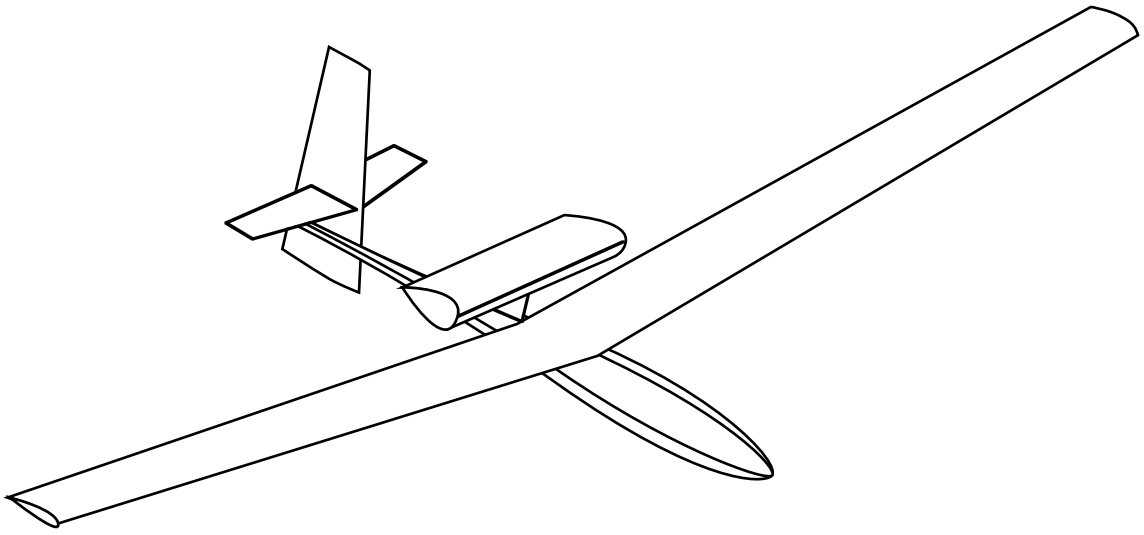

Figure 20. Strato7 configuration.

```
TRANSPORT
   4   2   2  570  570   0   0   0   2   1   7   0
  0.00010   0.6   10000.0
   1   2   3   6
   1   6
   1   6
*** GEOMETRY ***
 $FUS   BDMAX  = 3.00,     BODL   = 24.358,   FRAB   = 2.01
       FRN    = 2.15,     SFFACT = 1.082664,  ITAIL  = 1,
       OUTCOD = 3,        $END
 $WING  AR     = 23.328,   AREA   = 500.00,   DIHED  = 5.0,
       FDENWG = 0.0,      LFLAPC = 0.00,     SWEEP  = 0.00,
       SWFACT = 1.0,      TAPER  = 0.695,    TCROOT = 0.14,
       TCTIP  = 0.14,     TFLAPC = 0.0,      WFFRAC = 0.0,
       XWING  = 0.5664,   ZROOT  = 1.00,     KSWEEP = 2,
       $END
 $HTAIL  AR    = 5.96,     AREA   = 23.09,    SWEEP  = 5.00,
       SWFACT = 1.0,      TAPER  = 0.682,    TCROOT = 0.08,
       TCTIP  = 0.08,     XHTAIL = 1.25,     ZROOT  = 1.25,
       KSWEEP = 0,        SIZIT  = T,        HTFRAC = -0.20,
       CVHT   = -2.70560,  $END
 $VTAIL  AR    = 3.08,     AREA   = 17.69,    SWEEP  = 5.00,
       SWFACT = 1.00,     TAPER  = 0.554,    TCROOT = 0.08,
       TCTIP  = 0.08,     VTNO   = 1.0,      XVTAIL = 1.39,
       YROOT  = 0.00,     ZROOT  = 1.0,      KSWEEP = 0,
       SIZIT  = T,        VTFRAC = -0.20,    CVVT   = -0.59909,
       CGM    = 0.40,     $END
 $CREW   NCREW  = 0,        $END
 $FUEL   DEN    = 63.78,    FRAC   = 1.00,     $END
 $FPOD
  DIAM     =    2.,  LENGTH   =   2.,      X      =    0.592
  THETA    =    90.0,  SYMCOD   =    1,       SOD     =   -2,
  $END
$ENGINE N      = 1,        $END
$$$$$$$$$$$$$$$$$$$$$$$$$$$$$$$$$$$$$$$$$$$$$$$$$$$$$$$$$$$$$$$$$$$$$$$$$$$$$$$$$$$
 $TRDATA  CRMACH = .40,   QMAX   = 70.45,  DESLF  = 2.5,    ULTLF  = 3.75,
        WFUEL  = 392.0,  WFEXT  = 0.0,    WFTRAP = 0.1,    FRFURE = 0.0,
        IPSTO1 = 5,      TIMTO1 = 0.0,    IPSTO2 = 2,      TIMTO2 = 1.0,
        IPSLND = 5,      MODLND = 7,      VMRGLD = 1.2,    WKLAND = 0.1,
        IBREG  = 0,      IENDUR = 0,      WCOMBP = 0.6,    MMPROP = 7,
        NCODE  = 0,      NCRUSE = 1,      RANGE  = 100.0,  LENVEL =.FALSE.,
        NLEGCL = 30,     NLEGLO = 4,                  $END
       2
      MACH NO.   ALTITUDE    HORIZONTAL    NO.  VIND
PHASE   START END  START  END    DIST  TIME   TURN  "G"S  WKFUEL M IP IX W B A P
------- ---- ----  ----- -----  ------ -----  ---- -----  ------ - -- -- - - - -
CLIMB   .414   -1    100    -1     0.0   0.0   0.0    -1  1.0000 7 41  0 0 0 0 0
LOITER  .400   -1  90000    -1     0.0  10.0   0.0   0.0  1.0000 7 21  0 0 0 0 0

***** AERODYNAMICS *****
 $ACHAR  ABOSB=0.074, ALMAX=20.0, AMC=12.0, ALELJ=3, ISMNDR=0, SFWF=0.99,
       SMNSWP = 0.01, 0.10, 0.15, 0.20, 0.25, 0.30, 0.35, 0.40, 0.45, 0.51,
       CLOW   = 0.3821,0.3828,0.4266,0.4809,0.4849,0.4888,0.4946,0.5147,0.5502,0.5692,
       CMO    = -.1591,-.1596,-.1531,-.1466,-.1502,-.1538,-.1581,-.1653,-.1749,-.1823,
       $END
 $AMULT  FCDW=1.1, $END
 $ATRIM  FVCAM  = 0.9183,0.9244,0.9538,0.9196,0.9230,0.9276,0.9349,0.9345,0.9264,0.9247,
       FLDM   = 1.0211,1.0254,1.0200,1.0139,1.0200,1.0232,1.0234,1.0205,1.0226,0.8790,
       FLAPI  =  0.0,  0.0,  0.0,  0.0,  0.0,  0.0,  0.0,  0.0,  0.0,  0.0,
       ITRIM  =    1,    1,    1,    1,    1,    1,    1,    1,    1,    1,
       CGM=0.40, CFLAP=0.0, SPANF=0.0, IVCAM=1, ALFVC=5.0, $END
```

Figure 21. ACSYNT input for Strato7.

```
 $ADET   ICOD=1, IPLOT=1, NALF=10, NMDTL=10,
       ALIN=   -6.8, 0.0,  1.0,  2.0,  4.0,  6.0,  8.0, 10.0, 12.0, 14.0,
       ALTV   = 22740.,37475.,50131.,61224.,71097.,79992.,86129.,90000.,
       SMN    =  0.085, 0.119, 0.161, 0.210, 0.266, 0.328, 0.379, 0.400,
       ISTRS=    0,   0,   0,   0,   0,   0,   0,   0,   0,   0,
       ITB=      0,   0,   0,   0,   0,   0,   0,   0,   0,   0,
       ITS=      0,   0,   0,   0,   0,   0,   0,   0,   0,   0,
       $END
 $ADRAG  CDBMB=10*0.0,
       CDEXTR=10*0.0,
       CDTNK=10*0.00,
       $END
 $ATAKE  DELFLD=0.0, DELFTO=0.0, DELLED=0.0, DELLTO=0.0, ALFROT=8.0, $END
 $APRINT KERROR=2,   $END
Spark Ignition Internal Combustion Engine with Triple Turbocharging
 $PCONTR HNOUT  =     0.,31001.,50131.,79992.,90000.,
       SMNOUT =    0.0, 0.085, 0.161, 0.328, 0.400,
       NOUTPT = 5,         $END
 $PENGIN ENGNUM = 1,         NTPENG = 4,         ESZMCH = 0.00,
       ESZALT = 0.,        XNMAX  = 7200.0,    HPENG  = 115.0,
       SWTENG = 6.0,       HCRIT  = 90000.,    FSFC   = 1.0,
       $END
 $PROP   AF     = 125.0,     BL     = 2,         CLI    = 0.5,
       DPROP  = 17.88,     FPRW   = 0.087437,  FTHR   = 1.0,
       NTPPRP = 12,        PSZMCH = 0.00,      PSZALT = 0.,
       $END
 $PGEAR  GR     = 7.43,      ETR    = .95,       FGRW   = 0.2476234,
       GRSND  = 14.86,     $END
 $PENGNC XLENG  = 1.5,       RLENG  = 1.0,       DIA1   = 1.0,
       FT     = 0.0,       FRPN   = 1.0,       FRBT   = 2.0,
       NBDFT  = 0.3,       ANACHP = 0.,        DQ     = 0.024,
       $END
TRANSPORT
*** WEIGHTS ***
 $OPTS   WGTO = 3000.0, KERROR = 2,
       SLOPE(1)  = 0.47970,   TECHI(1) =    0.85,
       SLOPE(2)  = 0.97945,   TECHI(2) =    0.85,
       SLOPE(3)  = 0.64225,   TECHI(3) =    0.85,
       SLOPE(4)  = 0.85841,   TECHI(4) =    0.85,
       SLOPE(6)  = 0.70145,   TECHI(6) =    0.85,
       SLOPE(7)  = 0.85396,
       SLOPE(8)  = 0.55290,   TECHI(8) =    0.85,
       SLOPE(9)  = 1.89582,   TECHI(9) =    0.85,
       SLOPE(10) = 1.49618,
       SLOPE(11) = 0.19543,
       SLOPE(12) = 0.48091,
       SLOPE(13) = 3.68569,
       SLOPE(16) = 0.02254,
       SLOPE(17) = 1.0,
       KWING     =   6,
       KBODY     =   3,
       $END
 $FIXW   WE       = 757.5,
       WFEQ     =  0.,
       WFS      =  0.,
       WPL      =  0.,
 $END
```

Figure 21. Concluded.

```
$PDCYLIN

      PS=1.,          TMGW=.05,     EFFW=.605,
      EFFC=1.108,     ESW=12.9E06,  FCSW=75000.,   DSW=0.058,
      KDEW=1.0,       KDFW=1.0,
      ISTAMA=2,       CS1=0.01,     CS2=0.75,

      CLAQR=.001,     IFUEL=1,      CWMAN=1.0,     CF=6.25E-05,

      CKF=5.24,       EC=2.00,      KGC=.368,      KGW=.505,

      FTST = 4*58500.,8*0.,         FTSB = 4*58500.,8*0.,
      FCST = 4*54000.,8*0.,         FCSB = 4*54000.,8*0.,
      EST = 4*10.70E06,8*0.,        ESB = 4*10.70E06,8*0.,
      EFT = 4*30.0E06,8*0.,         EFB = 4*30.0E06,8*0.,
      DST = 4*.101,8*0.,            DSB = 4*.101,8*0.,
      DFT = 4*.292,8*0.,            DFB = 4*.292,8*0.,
      TMGT = 4*.03,8*0.,            TMGB = 4*.03,8*0.,
      KDE=0.9,                      KDF=0.8,
      CLBR1=1.1,                    ICYL = 1,

      KCONT = 12*4,                 KCONB = 12*4,

      AXAC=0.,        CBUM=1.0,     CLAN=0.93,
      CMAN=1.0,       ILOAD=3,      PGB = 12*11.5,  PGT = 12*11.5,
      WFBUMP=0.001,                 WFLAND=0.9,

      WTFF=0.07,

      VSINK=10.0,     STROKE=1.0,   CLRG1=.395,     CLRG2=0.5,
      WFGR1=0.0031,WFGR2=0.0058,    IGEAR=1,        GFRL=0.001,
      CLRGW1=0.20,  CLRGW2 = 0.0,

      ITAIL=1,

      ISCHRENK=1,   ICOMND=1,     WGNO=1.00,     SLFMB=1.2,
      WMIS=0.,      WSUR=0.,      WCW=1.0,       WCA=0.0,
      NWING=40,

$END
```

Figure 22. PDCYLIN namelist input for Strato7.

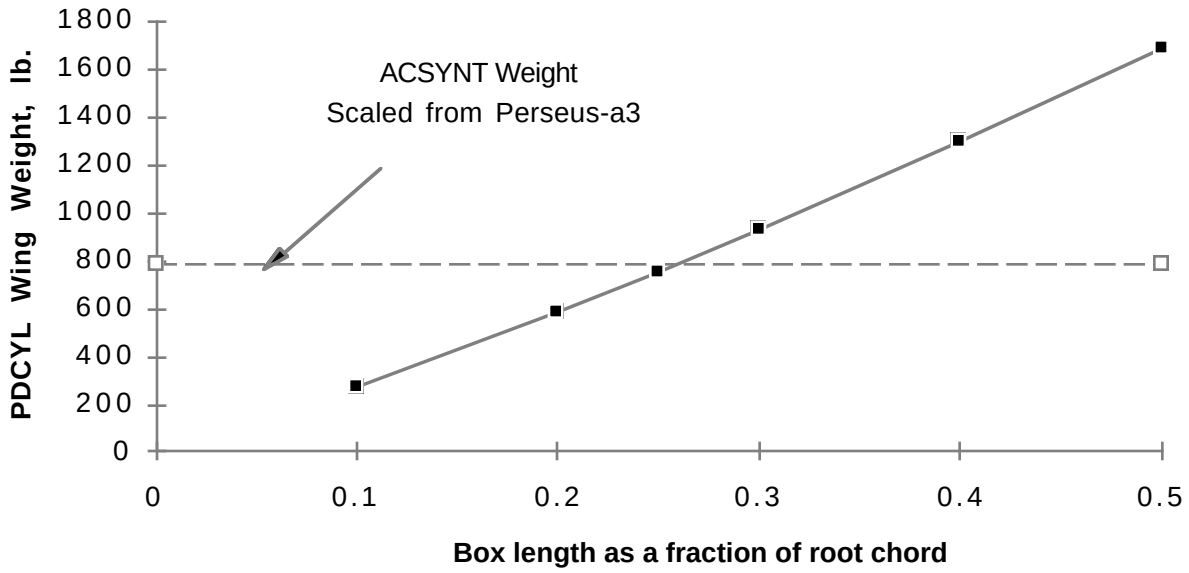

Figure 23. Strato7 wing weight as a function of structural box length.

References

1. Ardema, M. D.: Body Weight of Hypersonic Aircraft: Part 1. NASA TM-101028, Oct. 1988.
2. Ardema, M. D.; and Williams, L. J.: Transonic Transport Study − Structures and Aerodynamics, NASA TM X-62,157, May 1972.
3. Ardema, M. D.: Structural Weight Analysis of Hypersonic Aircraft. NASA TN D-6692, Mar. 1972.
4. Ardema, M. D.: Analysis of Bending Loads of Hypersonic Aircraft. NASA TM X-2092, 1970.
5. Moore, M.; and Samuels, J.: ACSYNT Aircraft Synthesis Program − User's Manual. Systems Analysis Branch, NASA Ames Research Center, Sept. 1990.
6. Shanley, F. R.: Weight-Strength Analysis of Aircraft Structures. Second Edition, Dover, N.Y., 1960.
7. Megson, T. H. G.: Aircraft Structures for Engineering Students. Second Edition, Halsted Press, 1990.
8. McCormick, B. W.: Aerodynamics, Aeronautics, and Flight Mechanics. John Wiley & Sons, 1979.
9. Crawford, R. F.; and Burns, A. B.: Strength, Efficiency, and Design Data for Beryllium Structures. ASD-TR-61-692, Feb. 1962.
10. Crawford, R. F.; and Burns, A. B.: Minimum Weight Potentials for Stiffened Plates and Shells. AIAA J., vol. 1, no. 4, Apr. 1963, pp. 879–886.
11. Popov, E. P.: Mechanics of Materials. Second Edition, Prentice-Hall, N.J., 1976.
12. Marquardt, D. W.: Least Squares Estimation of Nonlinear Parameters, a Computer Program in FORTRAN IV Language. IBM SHARE Library, Distribution Number 309401, Aug. 1966.
13. Niu, M. C.-Y.: Airframe Structural Design: Practical Design Information and Data on Aircraft Structures. Conmilit Press, 1991.
14. York, P.; and Labell, R. W.: Aircraft Wing Weight Build-Up Methodology with Modification for Materials and Construction Techniques. NASA CR-166173, Sept. 1980.
15. Thomas, R. B.; and Parsons, S. P.: Weight Data Base. The Boeing Company, Commercial Airplane Division, Weight Research Group, Doc. No. D6-23204 TN, 1968.
16. McDonnell Douglas Aircraft Company, Detailed Weight Statement for MD-11 Transport Aircraft, June 1987.
17. McDonnell Douglas Aircraft Company, Detailed Weight Statement for MD-80 Transport Aircraft, July 1991.

REPORT DOCUMENTATION PAGE

Form Approved
OMB No. 0704-0188

1. AGENCY USE ONLY *(Leave blank)*	2. REPORT DATE	3. REPORT TYPE AND DATES COVERED
	May 1996	Technical Memorandum

4. TITLE AND SUBTITLE

Analytical Fuselage and Wing Weight Estimation of Transport Aircraft

5. FUNDING NUMBERS

538-08-11

6. AUTHOR(S)

Mark D. Ardema,* Mark C. Chambers,* Anthony P. Patron,*
Andrew S. Hahn, Hirokazu Miura, and Mark D. Moore

7. PERFORMING ORGANIZATION NAME(S) AND ADDRESS(ES)

Ames Research Center
Moffett Field, CA 94035-1000

8. PERFORMING ORGANIZATION REPORT NUMBER

A-961451

9. SPONSORING/MONITORING AGENCY NAME(S) AND ADDRESS(ES)

National Aeronautics and Space Administration
Washington, DC 20546-0001

10. SPONSORING/MONITORING AGENCY REPORT NUMBER

NASA TM-110392

11. SUPPLEMENTARY NOTES

Point of Contact: Mark Ardema, Ames Research Center, MS 237-11, Moffett Field, CA 94035-1000
(415) 604-6651
*Santa Clara University, Santa Clara, California

12a. DISTRIBUTION/AVAILABILITY STATEMENT

Unclassified — Unlimited
Subject Category 05

12b. DISTRIBUTION CODE

13. ABSTRACT ***(Maximum 200 words)***

A method of estimating the load-bearing fuselage weight and wing weight of transport aircraft based on fundamental structural principles has been developed. This method of weight estimation represents a compromise between the rapid assessment of component weight using empirical methods based on actual weights of existing aircraft, and detailed, but time-consuming, analysis using the finite element method. The method was applied to eight existing subsonic transports for validation and correlation. Integration of the resulting computer program, PDCYL, has been made into the weights-calculating module of the AirCraft SYNThesis (ACSYNT) computer program. ACSYNT has traditionally used only empirical weight estimation methods; PDCYL adds to ACSYNT a rapid, accurate means of assessing the fuselage and wing weights of unconventional aircraft. PDCYL also allows flexibility in the choice of structural concept, as well as a direct means of determining the impact of advanced materials on structural weight.

Using statistical analysis techniques, relations between the load-bearing fuselage and wing weights calculated by PDCYL and corresponding actual weights were determined. A User's Manual and two sample outputs, one for a typical transport and another for an advanced concept vehicle, are given in the appendices.

14. SUBJECT TERMS	15. NUMBER OF PAGES
Structural analysis, Weight estimation, Transport aircraft	55
	16. PRICE CODE: A04

17. SECURITY CLASSIFICATION OF REPORT	18. SECURITY CLASSIFICATION OF THIS PAGE	19. SECURITY CLASSIFICATION OF ABSTRACT	20. LIMITATION OF ABSTRACT
Unclassified	Unclassified		